



Measurement of Λ_b^0 , Λ_c^+ and Λ decay parameters using $\Lambda_b^0 \rightarrow \Lambda_c^+ h^-$ decays

LHCb collaboration[†]

Abstract

A comprehensive study of the angular distributions in the bottom-baryon decays $\Lambda_b^0 \rightarrow \Lambda_c^+ h^-$ ($h = \pi, K$), followed by $\Lambda_c^+ \rightarrow \Lambda h^+$ with $\Lambda \rightarrow p\pi^-$ or $\Lambda_c^+ \rightarrow pK_S^0$ decays, is performed using a data sample of proton-proton collisions corresponding to an integrated luminosity of 9 fb^{-1} collected by the LHCb experiment at center-of-mass energies of 7, 8 and 13 TeV. The decay parameters and the associated charge-parity (CP) asymmetries are measured, with no significant CP violation observed. For the first time, the $\Lambda_b^0 \rightarrow \Lambda_c^+ h^-$ decay parameters are measured. The most precise measurements of the decay parameters α, β and γ are obtained for Λ_c^+ decays and an independent measurement of the decay parameters for the strange-baryon Λ decay is provided. The results deepen our understanding of weak decay dynamics in baryon decays.

Submitted to Phys. Rev. Lett.

© 2024 CERN for the benefit of the LHCb collaboration. CC BY 4.0 licence.

[†]Authors are listed at the end of this paper.

Hadronic weak decays of baryons provide an excellent platform for studying baryon decay dynamics and the origin of the asymmetry between matter and antimatter [1–3]. Among them, the decay of a spin-half baryon to a spin-half baryon and a pseudoscalar meson is of special interest. For this type of decay, three decay parameters, first proposed by Lee and Yang to search for parity violation [4], can be defined as

$$\alpha \equiv \frac{2\Re(s^*p)}{|s|^2 + |p|^2}, \quad \beta \equiv \frac{2\Im(s^*p)}{|s|^2 + |p|^2}, \quad \gamma \equiv \frac{|s|^2 - |p|^2}{|s|^2 + |p|^2}, \quad (1)$$

satisfying $\alpha^2 + \beta^2 + \gamma^2 = 1$, where s and p denote the parity-violating S-wave and parity-conserving P-wave amplitudes, respectively. The interference between the two amplitudes may generate differences between the differential decay rates of baryons and antibaryons, allowing CP -violation phenomena to be probed via angular analyses [5]. The amount of CP violation can be quantified by the asymmetries $A_\alpha = (\alpha + \bar{\alpha})/(\alpha - \bar{\alpha})$ and $R_\beta = (\beta + \bar{\beta})/(\alpha - \bar{\alpha})$, where $\bar{\alpha}$ and $\bar{\beta}$ denote the decay parameters of the antibaryons, and should have signs opposite to their baryonic counterparts. At leading order, these CP asymmetries are related to the weak and strong phase differences between the S- and P-wave amplitudes, $\Delta\phi$ and $\Delta\delta$, via the relations $A_\alpha = -\tan\Delta\delta \tan\Delta\phi$ and $R_\beta = \tan\Delta\phi$ [1].

Many phenomenological models have been used to calculate baryon decay parameters. For some two-body beauty-baryon decays, factorization is assumed to hold in model calculations [6–15], which predict that $\alpha \approx -1$, consistent with the $V - A$ nature of the weak current and maximal parity violation. For charm-baryon decays, model calculations are complicated by the presence of nonfactorizable contributions and often do not agree with each other [16–27]. For strange-baryon decays, nonfactorizable contributions may dominate, making theoretical calculations even more challenging [1].

Decay parameters have been measured for several hyperon and charm-baryon decays [28], while beauty decays are much less explored. The α parameter of the $\Lambda \rightarrow p\pi^-$ decay was recently updated by the BESIII [29, 30] and CLAS [31] collaborations, which resulted in a significantly larger value compared to the previous world average [32]. The α parameters of several Λ_c^+ decays were precisely measured by the FOCUS [33], BESIII [34] and Belle [35] collaborations, while the precision of the β and γ measurements is still very limited [34, 36]. To date, there is no decay parameter measurement for any Λ_b^0 decay to a baryon and a pseudoscalar meson, despite the observation of many such decay modes. The decay parameter of the $\Lambda_b^0 \rightarrow J/\psi\Lambda$ decay was measured in proton-proton (pp) collisions at the LHC [37–40], together with the Λ_b^0 polarization, which is found to be consistent with zero. Moreover, the photon polarization of the $\Lambda_b^0 \rightarrow \Lambda\gamma$ decay was measured by LHCb [41], suggesting the dominance of left-handed photons.

In this Letter, the decay parameters and CP asymmetries of $\Lambda_b^0 \rightarrow \Lambda_c^+\pi^-$ and $\Lambda_b^0 \rightarrow \Lambda_c^+K^-$ decays are measured through an angular analysis. Three Λ_c^+ decays are analyzed: $\Lambda_c^+ \rightarrow pK_S^0$, $\Lambda_c^+ \rightarrow \Lambda\pi^+$ and $\Lambda_c^+ \rightarrow \Lambda K^+$ with the subsequent decays $\Lambda \rightarrow p\pi^-$ and $K_S^0 \rightarrow \pi^+\pi^-$. The decay parameters and associated CP asymmetries of the Λ_b^0 , Λ_c^+ and Λ decays are determined simultaneously. The analysis is performed using data from pp collisions at center-of-mass energies of $\sqrt{s} = 7, 8$ and 13 TeV, corresponding to an integrated luminosity of 9 fb^{-1} collected with the LHCb detector. Inclusion of charge-conjugate processes is implied, unless otherwise stated.

The LHCb detector, designed for the study of particles containing b or c quarks, is a single-arm forward spectrometer covering the pseudorapidity range $2 < \eta < 5$, described in detail in Refs. [42, 43]. The online event selection for Λ_b^0 decays is performed by a

trigger [44], which consists of a hardware stage followed by a software stage [45–48]. The hardware trigger requires a muon with high transverse momentum or a hadron, photon or electron with high transverse energy in the calorimeters. The software trigger requires a two-, three- or four-track secondary vertex with a significant displacement from any primary vertex (PV).

Simulated samples of Λ_b^0 decays are produced to optimize event selection, study potential backgrounds and model the detector acceptance. These samples are generated using the software described in Refs. [49–54]. The products of each decay in the Λ_b^0 cascades are distributed uniformly in the allowed phase space.

In the offline selection, all tracks in the final state are required to have a large transverse momentum and be inconsistent with being directly produced from any PV. The Λ and K_S^0 candidates are reconstructed using $\Lambda \rightarrow p\pi^-$ and $K_S^0 \rightarrow \pi^-\pi^+$ decays, where the final-state tracks are required to form a vertex with a good fit quality that is significantly displaced from any PV, and their invariant mass is consistent with the known value [28]. The Λ (K_S^0) candidate is combined with a kaon/pion (proton) track to form the Λ_c^+ candidate. The Λ_c^+ invariant mass is required to be within ± 26 (20) MeV/c^2 of the known value [28] for the $\Lambda_c^+ \rightarrow pK_S^0$ and $\Lambda_c^+ \rightarrow \Lambda\pi^+$ ($\Lambda_c^+ \rightarrow \Lambda K^+$) decays. The smaller mass region for the $\Lambda_c^+ \rightarrow \Lambda K^+$ decay is used to suppress the $\Lambda_c^+ \rightarrow \Sigma^0(\rightarrow \Lambda\gamma)\pi^+$ background, where the photon is not reconstructed. The Λ_b^0 candidate is formed by combining a Λ_c^+ candidate with a kaon or pion. The Λ_b^0 invariant mass, $m(\Lambda_c^+h^-)$, is required to be larger than $5500 \text{ MeV}/c^2$ to reject background due to partially reconstructed Λ_b^0 decays.

Two types of background peaking in the signal mass region are identified. For the first type, D^0 or J/ψ mesons are observed in the invariant-mass distributions of the two charged companion tracks of Λ_b^0 and Λ_c^+ decays. The second type involves a genuine K_S^0 (Λ) decay reconstructed as the Λ (K_S^0) decay. These background candidates are suppressed using information from particle identification (PID) detectors or rejected by specific vetoes in the corresponding mass spectra. A boosted decision tree (BDT) classifier implemented in the TMVA toolkit [55] is then used to separate the Λ_b^0 signal from the background of random combinations of final-state particles. The BDT analysis is performed independently for $\Lambda_c^+ \rightarrow pK_S^0$ and $\Lambda_c^+ \rightarrow \Lambda h^+$ decays. Each BDT classifier is trained on simulated signal decays and background from data in the high-mass region $m(\Lambda_c^+h^-) > 5900 \text{ MeV}/c^2$, using a combination of kinematic, topological and isolation variables of the Λ_b^0 , Λ_c^+ , Λ or K_S^0 hadrons. In the final stage of the event selection, a simultaneous optimization of the final-state PID and BDT classifier requirements is performed to maximize the figure of merit, $N_S^2/(N_S + N_B)^{3/2}$, chosen to favour a high signal purity with small decay-parameter uncertainties. Here, N_S and N_B represent the signal and background yields in the signal region chosen to be $\pm 32 \text{ MeV}/c^2$ around the known Λ_b^0 mass [28], estimated with simulated signal decays and data in the high-mass region. The Λ_b^0 invariant mass is calculated with a kinematic fit [56] constraining the masses of all intermediate particles to their known values and the Λ_b^0 momentum to point back to its best-matched PV.

The invariant-mass distributions of the five significant Λ_b^0 cascade decays to $(pK_S^0)\pi^-$, $(pK_S^0)K^-$, $(\Lambda\pi^+)\pi^-$, $(\Lambda\pi^+)K^-$ and $(\Lambda K^+)\pi^-$ final states, where Λ_c^+ decay products are shown in brackets, are shown in Fig. 1 for candidates passing all selection criteria. The signal yields of the five decays are determined to be $(8.635 \pm 0.032) \times 10^4$, $(4.16 \pm 0.07) \times 10^3$, $(2.475 \pm 0.017) \times 10^4$, $(1.19 \pm 0.04) \times 10^3$ and $(1.010 \pm 0.034) \times 10^3$, respectively, from unbinned maximum-likelihood fits performed to the Λ_b^0 mass distributions. The signal component is described by a Hypatia function [57] and the combinatorial background by

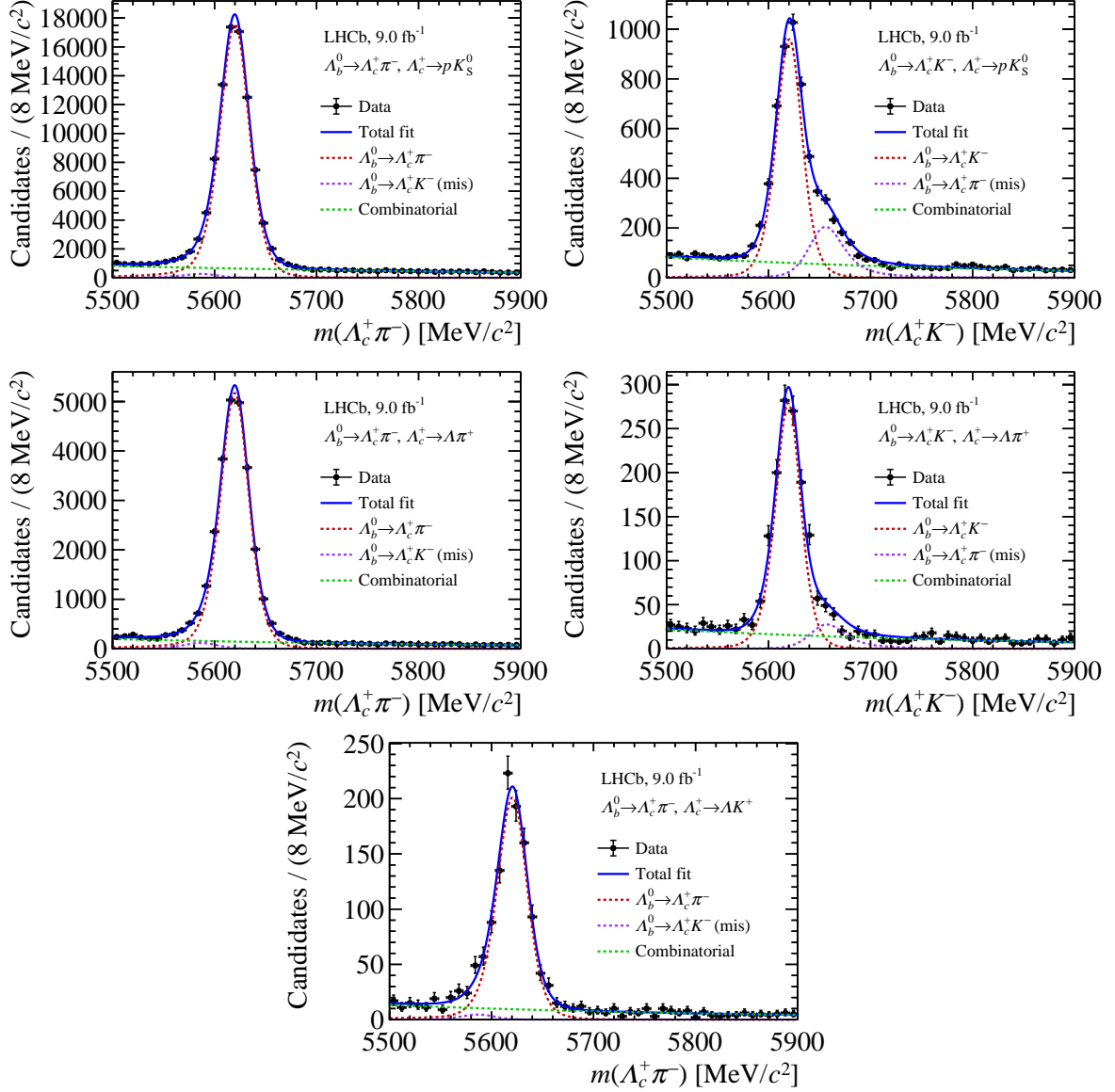


Figure 1: The invariant-mass distributions of Λ_b^0 candidates reconstructed in the (top left) $\Lambda_b^0 \rightarrow \Lambda_c^+ (\rightarrow p K_S^0) \pi^-$, (top right) $\Lambda_b^0 \rightarrow \Lambda_c^+ (\rightarrow p K_S^0) K^-$, (middle left) $\Lambda_b^0 \rightarrow \Lambda_c^+ (\rightarrow \Lambda \pi^+) \pi^-$, (middle right) $\Lambda_b^0 \rightarrow \Lambda_c^+ (\rightarrow \Lambda \pi^+) K^-$ and (bottom) $\Lambda_b^0 \rightarrow \Lambda_c^+ (\rightarrow \Lambda K^+) \pi^-$ decays, with the fit results drawn.

an exponential function. The $\Lambda_b^0 \rightarrow \Lambda_c^+ K^-$ decay misidentified as $\Lambda_b^0 \rightarrow \Lambda_c^+ \pi^-$ decay, or vice versa, is also modelled by a Hypatia function, whose parameters are fixed to those obtained from the simulated samples. The relative yields of these cross-feed contributions are constrained using relative experimental efficiencies. For every decay mode, the fit result is used to determine the *sPlot* weight for each candidate [58], applied to subtract the background for the subsequent angular analysis.

The decay parameters are determined by analyzing the angular distributions of the Λ_b^0 cascade decays. The angular variables are calculated with the Λ_b^0 invariant mass constrained to the known value [28]. The kinematics of the three-step cas-

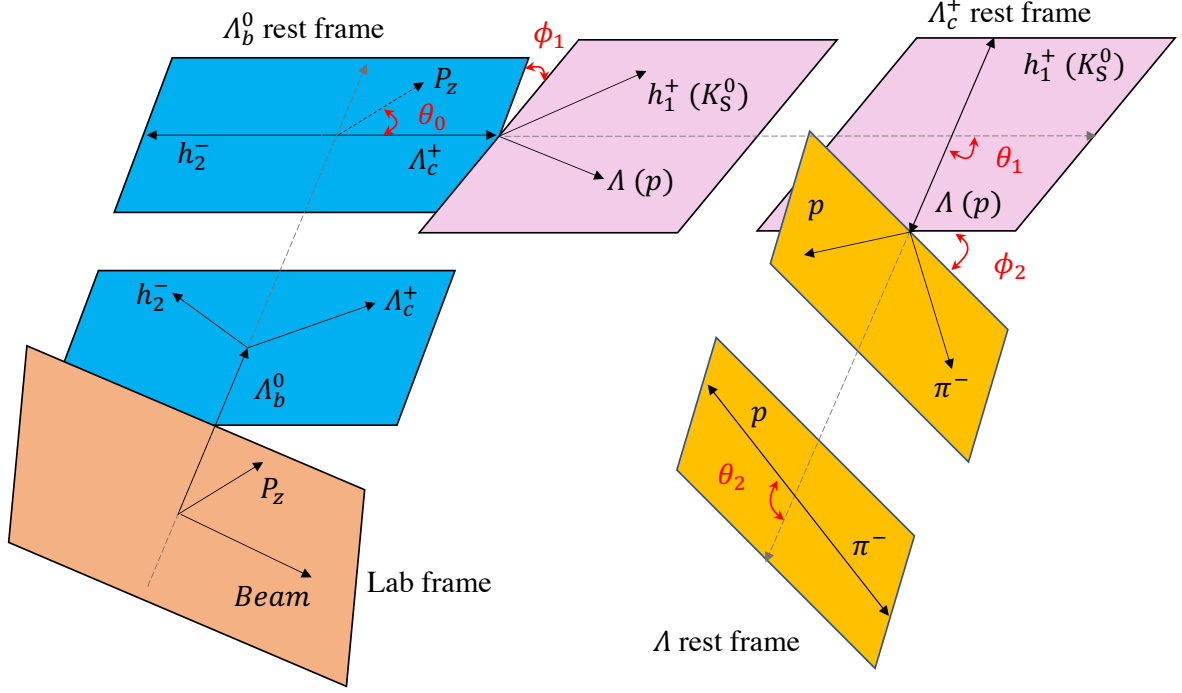


Figure 2: Definition of the helicity angles for $\Lambda_b^0 \rightarrow (\Lambda_c^+ \rightarrow \Lambda h_1^+) h_2^-$ and $\Lambda_b^0 \rightarrow (\Lambda_c^+ \rightarrow p K_S^0) h_2^-$ decays, where h_1^+, h_2^- denote the kaon or pion.

cade $\Lambda_b^0 \rightarrow \Lambda_c^+ (\rightarrow \Lambda (\rightarrow p \pi^-) h_1^+) h_2^-$ decays are fully described by five angular variables $\vec{\Omega} \equiv (\theta_0, \theta_1, \phi_1, \theta_2, \phi_2)$, depicted in Fig. 2. The variable θ_0 is the polar angle between the normal \vec{P}_z of the production plane formed by the beam and Λ_b^0 momenta in the laboratory frame, and the Λ_c^+ momentum $\vec{p}_{\Lambda_c^+}$ in the Λ_b^0 rest frame. The variable θ_1 (θ_2) is the polar angle between $\vec{p}_{\Lambda_c^+}$ (\vec{p}_p) and \vec{p}_Λ , where particle momenta are defined in the rest frames of the Λ_b^0 (Λ) and Λ_c^+ baryons, respectively. The variable ϕ_1 (ϕ_2) is the angle between the Λ_b^0 (Λ) decay plane and the Λ_c^+ decay plane, spanned by the momenta of their respective decay products. Similarly, for the two-step cascade decays, $\Lambda_b^0 \rightarrow \Lambda_c^+ (\rightarrow p K_S^0) h_2^-$, the kinematics are described by three angular variables $\vec{\Omega} \equiv (\theta_0, \theta_1, \phi_1)$, which are the same as the first three variables of the three-step cascade.

The angular distributions can be expanded through the helicity formalism [59]. Based on previous studies at the LHC [37–40], the Λ_b^0 baryon is considered to be unpolarized, in which case the angular distributions become uniform in θ_0 and ϕ_1 . The impact of Λ_b^0 polarization is considered as a source of systematic uncertainty. The reduced angular distributions are thus expressed as

$$\begin{aligned} \frac{d^3\Gamma}{d\cos\theta_1 d\cos\theta_2 d\phi_2} \propto & (1 + \alpha_{\Lambda_b^0} \alpha_{\Lambda_c^+} \cos\theta_1 + \alpha_{\Lambda_c^+} \alpha_\Lambda \cos\theta_2 + \alpha_{\Lambda_b^0} \alpha_\Lambda \cos\theta_1 \cos\theta_2 \\ & - \alpha_{\Lambda_b^0} \gamma_{\Lambda_c^+} \alpha_\Lambda \sin\theta_1 \sin\theta_2 \cos\phi_2 + \alpha_{\Lambda_b^0} \beta_{\Lambda_c^+} \alpha_\Lambda \sin\theta_1 \sin\theta_2 \sin\phi_2), \end{aligned} \quad (2)$$

for $\Lambda_b^0 \rightarrow \Lambda_c^+ (\rightarrow \Lambda (\rightarrow p \pi^-) h_1^+) h_2^-$ decays, and

$$\frac{d\Gamma}{d\cos\theta_1} \propto 1 + \alpha_{\Lambda_b^0} \alpha_{\Lambda_c^+} \cos\theta_1, \quad (3)$$

for $\Lambda_b^0 \rightarrow \Lambda_c^+(\rightarrow pK_S^0)h_2^-$ decays, where the subscript of the decay parameters denotes the decaying particle. The decay parameters in this analysis are determined from simultaneous unbinned maximum-likelihood fits to the five Λ_b^0 ($\bar{\Lambda}_b^0$) cascade decays, imposing the constraint $(\alpha_{\Lambda_c^+})^2 + (\beta_{\Lambda_c^+})^2 + (\gamma_{\Lambda_c^+})^2 = 1$. The $\beta_{\Lambda_c^+}$ and $\gamma_{\Lambda_c^+}$ parameters are related to the $\alpha_{\Lambda_c^+}$ and $\Delta_{\Lambda_c^+}$ parameters by $\beta_{\Lambda_c^+} = \sqrt{1 - (\alpha_{\Lambda_c^+})^2} \sin \Delta_{\Lambda_c^+}$, $\gamma_{\Lambda_c^+} = \sqrt{1 - (\alpha_{\Lambda_c^+})^2} \cos \Delta_{\Lambda_c^+}$, where $\Delta_{\Lambda_c^+}$ is the phase difference between the two helicity amplitudes of the $\Lambda_c^+ \rightarrow \Lambda h^+$ decay. This leads to two equivalent sets of fit parameters for a $\Lambda_c^+ \rightarrow \Lambda h^+$ decay. The fit is performed for each set of parameters independently to directly determine their values and uncertainties. To test CP violation, an additional joint fit of Λ_b^0 and $\bar{\Lambda}_b^0$ samples is applied with CP -related fit parameters, which are the CP asymmetries A_α , R_β , and CP averages $\langle \alpha \rangle \equiv (\alpha - \bar{\alpha})/2$, $R'_\beta \equiv (\beta - \bar{\beta})/(\alpha - \bar{\alpha})$. At leading order, the weak and strong phase differences are determined using $R_\beta = \tan \Delta\phi$ and $R'_\beta = \tan \Delta\delta$ [1].

The logarithm of the likelihood function ($\log \mathcal{L}$) is constructed as

$$\log \mathcal{L}(\vec{\nu}) = \sum_{k=1}^5 \left(\mathcal{C}_k \sum_{i=1}^{N_k} w_{k,i} \times \log \left[\mathcal{P}_k(\vec{\Omega}_k^i | \vec{\nu}) \right] \right), \quad (4)$$

where $\vec{\nu}$ is the set of decay parameters, $\vec{\Omega}$ is the set of angular variables, and $\mathcal{P}(\vec{\Omega} | \vec{\nu})$ represents the signal probability density function (PDF). The subscript k runs over the five Λ_b^0 cascade decays, and the subscript i runs over all the N_k candidates of the k -th decay. The $sPlot$ weight $w_{k,i}$ in the $\log \mathcal{L}$ is used to remove the contribution of background candidates [58], while the constants $\mathcal{C}_k \equiv \sum_{i \in \text{data}_k} w_{k,i} / \sum_{i \in \text{data}_k} w_{k,i}^2$ are scale factors needed to correct the obtained statistical uncertainties [60]. The signal PDF $\mathcal{P}_k(\vec{\Omega}_k | \vec{\nu})$ is formulated as

$$\mathcal{P}_k(\vec{\Omega}_k | \vec{\nu}) = \frac{\epsilon_k(\vec{\Omega}_k) \cdot f_k(\vec{\Omega}_k | \vec{\nu})}{\int d\vec{\Omega}_k \epsilon_k(\vec{\Omega}_k) \cdot f_k(\vec{\Omega}_k | \vec{\nu})}, \quad (5)$$

where $f_k(\vec{\Omega}_k | \vec{\nu})$ represents the angular distribution given in Eq. 2 or 3, and $\epsilon_k(\vec{\Omega}_k)$ is the angular acceptance. The denominator is calculated numerically using the Monte Carlo integration method [61] beginning with the corresponding simulated signal decays after full selection. The distributions of the Λ_b^0 transverse momentum and pseudorapidity, and the number of tracks per event in the simulation samples are corrected to match those in data. In Fig. 3, the angular distributions of $\Lambda_b^0 \rightarrow \Lambda_c^+(\rightarrow pK_S^0)h^-$ and $\Lambda_b^0 \rightarrow \Lambda_c^+(\rightarrow \Lambda h^+)\pi^-$ decays are shown, superimposed by the fit result. Distributions for all decays are provided in Ref. [62]. A binned χ^2 test between the data and the fit gives a p-value of 28%.

Various sources of systematic uncertainty on the decay parameters are studied. Possible biases introduced by the angular fit method are evaluated using pseudoexperiments. Mass and angular distributions of pseudosamples are generated according to the baseline fit results, and then the whole fit procedure is repeated to extract decay parameters. The parameter's systematic uncertainty is taken to be the mean of its pull distribution times its nominal statistical uncertainty. The $sPlot$ method is used to subtract the background, hence the choice of the invariant-mass fit model introduces systematic uncertainties. These are estimated by repeating the invariant-mass fit with alternative fit models, including alternative descriptions of mass-shape functions and removing the constraints on yields, then using the corresponding updated $sPlot$ weights to determine decay parameters. As the PID variables in simulation samples are calibrated to match data [63, 64], the uncertainty

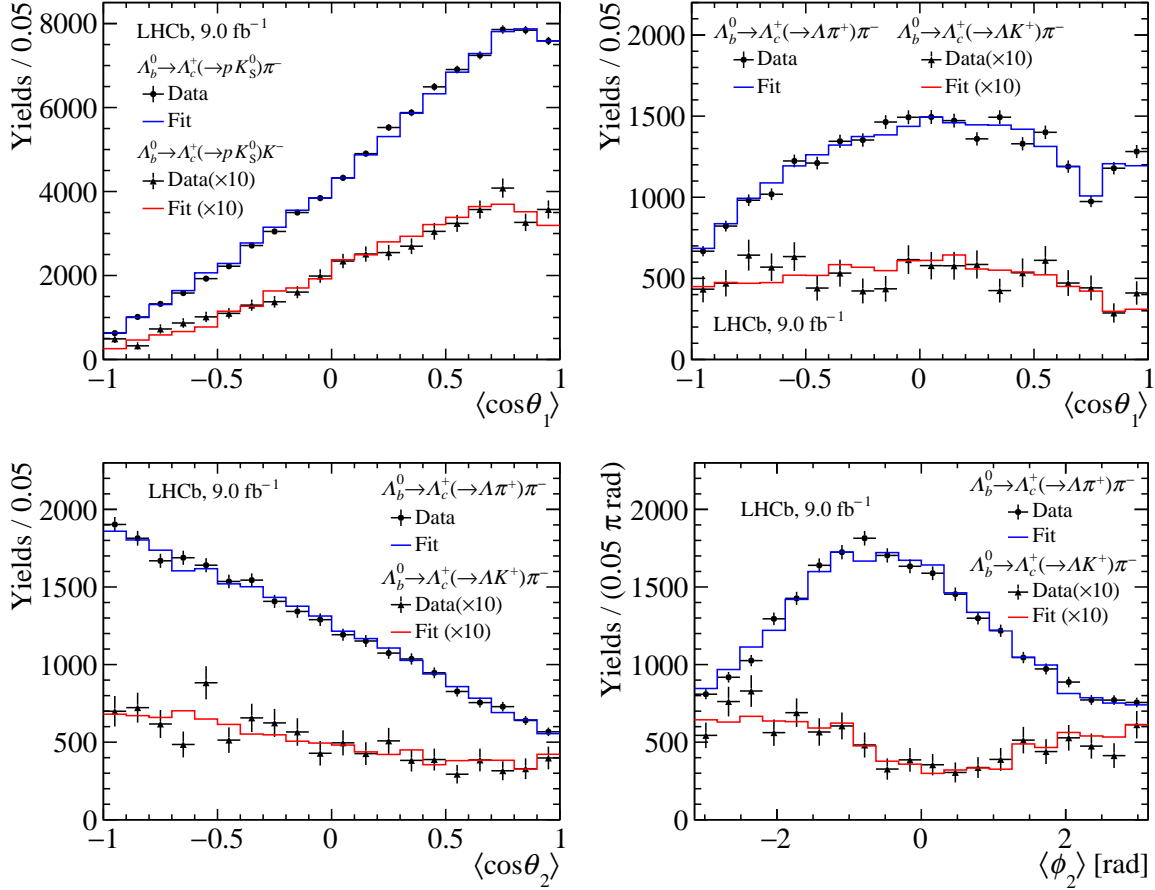


Figure 3: Distributions of (top left) the $\langle \cos \theta_1 \rangle$ angle of the $\Lambda_b^0 \rightarrow \Lambda_c^+ (\rightarrow p K_S^0) h^-$ decays, and the (top right) $\langle \cos \theta_1 \rangle$, (bottom left) $\langle \cos \theta_2 \rangle$ and (bottom right) $\langle \phi_2 \rangle$ angles of the $\Lambda_b^0 \rightarrow \Lambda_c^+ (\rightarrow \Lambda h^+) \pi^-$ decays. The angular brackets denote that the Λ_b^0 and $\bar{\Lambda}_b^0$ samples are merged, where the ϕ_2 signs are also flipped for $\bar{\Lambda}_b^0$ samples. Points with error bars correspond to background-subtracted data using the *sPlot* technique.

on the calibration procedure introduces systematic uncertainties which are estimated with alternative calibration configurations. The limited size of simulation samples introduces an uncertainty on the efficiency propagated to the decay parameters, which is estimated with bootstrapped pseudoexperiments [65]. The influence of the production asymmetry for Λ_b^0 baryons and detection asymmetries on the final-state particles [66–68] are taken into account. Following the prescription of CP measurements [69, 70], these asymmetries are introduced in the angular acceptance, and the angular fit is repeated to verify their impact on the measurements. The polarization of Λ_b^0 baryons is considered as a source of systematic uncertainty. The angular fit is repeated with additional terms in the PDF incorporating the transverse polarization measured by LHCb [38] (see appendix for details on this PDF). The impact of the experimental angular resolution is considered as a systematic uncertainty and found to be negligible. The spin of the Λ baryon undergoes a precession in the magnetic field of the detector, which modifies its angular distribution depending on the decay length [71]. The systematic uncertainty arising from the precession is examined using pseudoexperiments, and found to be negligible. A summary of the

Table 1: Measurements of α parameters and their CP asymmetries for $\Lambda_b^0 \rightarrow \Lambda_c^+ \pi^-$, $\Lambda_b^0 \rightarrow \Lambda_c^+ K^-$, $\Lambda_c^+ \rightarrow \Lambda \pi^+$, $\Lambda_c^+ \rightarrow \Lambda K^+$, $\Lambda_c^+ \rightarrow p K_S^0$ and $\Lambda \rightarrow p \pi^-$ decays. The first uncertainties are statistical and the second are systematic.

Decay	α	$\bar{\alpha}$	$\langle \alpha \rangle$	A_α
$\Lambda_b^0 \rightarrow \Lambda_c^+ \pi^-$	$-1.010 \pm 0.011 \pm 0.003$	$0.996 \pm 0.011 \pm 0.003$	$-1.003 \pm 0.008 \pm 0.005$	$0.007 \pm 0.008 \pm 0.005$
$\Lambda_b^0 \rightarrow \Lambda_c^+ K^-$	$-0.933 \pm 0.042 \pm 0.014$	$0.995 \pm 0.036 \pm 0.013$	$-0.964 \pm 0.028 \pm 0.015$	$-0.032 \pm 0.029 \pm 0.006$
$\Lambda_c^+ \rightarrow \Lambda \pi^+$	$-0.782 \pm 0.009 \pm 0.004$	$0.787 \pm 0.009 \pm 0.003$	$-0.785 \pm 0.006 \pm 0.003$	$-0.003 \pm 0.008 \pm 0.002$
$\Lambda_c^+ \rightarrow \Lambda K^+$	$-0.569 \pm 0.059 \pm 0.028$	$0.464 \pm 0.058 \pm 0.017$	$-0.516 \pm 0.041 \pm 0.021$	$0.102 \pm 0.080 \pm 0.023$
$\Lambda_c^+ \rightarrow p K_S^0$	$-0.744 \pm 0.012 \pm 0.009$	$0.765 \pm 0.012 \pm 0.007$	$-0.754 \pm 0.008 \pm 0.006$	$-0.014 \pm 0.011 \pm 0.008$
$\Lambda \rightarrow p \pi^-$	$0.717 \pm 0.017 \pm 0.009$	$-0.748 \pm 0.016 \pm 0.007$	$0.733 \pm 0.012 \pm 0.006$	$-0.022 \pm 0.016 \pm 0.007$

Table 2: Measurements of the decay parameters β and γ , the phase difference Δ , the CP asymmetry R_β and the CP average R'_β for $\Lambda_c^+ \rightarrow \Lambda \pi^+$, $\Lambda_c^+ \rightarrow \Lambda K^+$ decays and their charge-conjugated decays. The first uncertainties are statistical and the second are systematic.

Decay	$\Lambda_c^+ \rightarrow \Lambda \pi^+$	$\Lambda_c^+ \rightarrow \Lambda K^+$
β	$0.368 \pm 0.019 \pm 0.008$	$0.35 \pm 0.12 \pm 0.04$
$\bar{\beta}$	$-0.387 \pm 0.018 \pm 0.010$	$-0.32 \pm 0.11 \pm 0.03$
γ	$0.502 \pm 0.016 \pm 0.006$	$-0.743 \pm 0.067 \pm 0.024$
$\bar{\gamma}$	$0.480 \pm 0.016 \pm 0.007$	$-0.828 \pm 0.049 \pm 0.013$
Δ (rad)	$0.633 \pm 0.036 \pm 0.013$	$2.70 \pm 0.17 \pm 0.04$
$\bar{\Delta}$ (rad)	$-0.678 \pm 0.035 \pm 0.013$	$-2.78 \pm 0.13 \pm 0.03$
R_β	$0.012 \pm 0.017 \pm 0.005$	$-0.04 \pm 0.15 \pm 0.02$
R'_β	$-0.481 \pm 0.019 \pm 0.009$	$-0.65 \pm 0.17 \pm 0.07$

contributions from the various sources is given in Ref. [62]. The systematic uncertainties from different sources are added in quadrature, resulting in totals that are smaller than the statistical uncertainties.

The results are listed in Table 1 for the α parameters of Λ_b^0 , Λ_c^+ and Λ decays, and in Table 2 for the β and γ parameters of $\Lambda_c^+ \rightarrow \Lambda h^+$ decays. The CP -related parameters are also obtained, and no CP violation is found. This is the first measurement of the parity-violating parameters of two-body Λ_b^0 decays into a spin-half baryon and a pseudoscalar meson. The results of the $\alpha_{\Lambda_b^0}$ decay parameters are close to -1 , suggesting that Λ_c^+ baryons in $\Lambda_b^0 \rightarrow \Lambda_c^+ h^-$ decays are almost fully longitudinally polarized, which corresponds to the $V - A$ nature of weak decays and supports the factorization hypothesis in theoretical calculations [72]. The Λ_c^+ decay parameters are consistent with, and more precise than, the Belle [35] and BESIII [34] results. The $\alpha_{\Lambda_c^+}$ parameters are found to significantly deviate from -1 , which may suggest that nonfactorizable contributions are substantial in hadronic decays of charm baryons. The β, γ and Δ parameters of $\Lambda_c^+ \rightarrow \Lambda h^+$ decays are precisely measured for the first time, and will serve as essential inputs to theoretical models [73]. The weak and strong phase differences are determined to be $\Delta\phi = 0.01 \pm 0.02$ rad and $\Delta\delta = -0.448 \pm 0.017$ rad for the $\Lambda_c^+ \rightarrow \Lambda \pi^+$ decay, and $\Delta\phi = -0.03 \pm 0.15$ rad and $\Delta\delta = -0.57 \pm 0.19$ rad for the $\Lambda_c^+ \rightarrow \Lambda K^+$ decay, where a possible ambiguity of $+\pi$ rad due to the inverse of tangent function is not included. The α parameter and the corresponding CP asymmetry of the $\Lambda \rightarrow p \pi^-$ decay in this analysis are consistent with the BESIII results [29, 30].

In conclusion, based on pp collision data collected by the LHCb experiment, corresponding to an integrated luminosity of 9 fb^{-1} , a comprehensive study of the angular distributions in Λ_b^0 cascade decays is performed. The analysis provides the first measurements of the decay parameters for $\Lambda_b^0 \rightarrow \Lambda_c^+ h^-$ decays, and the most precise measurements for the Λ_c^+ decay parameters. The weak and strong phase differences for $\Lambda_c^+ \rightarrow \Lambda h^+$ decays are also determined. The CP asymmetries are studied between the decay parameters of baryon and antibaryon decays, and no hint of CP violation is observed. The results provide valuable insights into the weak decay dynamics of baryons.

Acknowledgements

We express our gratitude to our colleagues in the CERN accelerator departments for the excellent performance of the LHC. We thank the technical and administrative staff at the LHCb institutes. We acknowledge support from CERN and from the national agencies: CAPES, CNPq, FAPERJ and FINEP (Brazil); MOST and NSFC (China); CNRS/IN2P3 (France); BMBF, DFG and MPG (Germany); INFN (Italy); NWO (Netherlands); MNiSW and NCN (Poland); MCID/IFA (Romania); MICIU and AEI (Spain); SNSF and SER (Switzerland); NASU (Ukraine); STFC (United Kingdom); DOE NP and NSF (USA). We acknowledge the computing resources that are provided by CERN, IN2P3 (France), KIT and DESY (Germany), INFN (Italy), SURF (Netherlands), PIC (Spain), GridPP (United Kingdom), CSCS (Switzerland), IFIN-HH (Romania), CBPF (Brazil), and Polish WLCG (Poland). We are indebted to the communities behind the multiple open-source software packages on which we depend. Individual groups or members have received support from ARC and ARDC (Australia); Key Research Program of Frontier Sciences of CAS, CAS PIFI, CAS CCEPP, Fundamental Research Funds for the Central Universities, and Sci. & Tech. Program of Guangzhou (China); Minciencias (Colombia); EPLANET, Marie Skłodowska-Curie Actions, ERC and NextGenerationEU (European Union); A*MIDEX, ANR, IPhU and Labex P2IO, and Région Auvergne-Rhône-Alpes (France); AvH Foundation (Germany); ICSC (Italy); Severo Ochoa and María de Maeztu Units of Excellence, GVA, XuntaGal, GENCAT, InTalent-Inditex and Prog. Atracción Talento CM (Spain); SRC (Sweden); the Leverhulme Trust, the Royal Society and UKRI (United Kingdom).

End matter

1 Angular distributions

The helicity formalism is employed to describe the angular distributions of the decays in this Letter. For the decay of a spin-half baryon to a spin-half baryon and a pseudoscalar meson, two helicity amplitudes are involved with the respective couplings H_{\pm} , where the subscript represents the sign of the helicity of the final-state spin-half baryon. The helicity couplings are related to the S-wave (s) and P-wave (p) couplings as $s = (H_+ + H_-)/\sqrt{2}$ and $p = (H_+ - H_-)/\sqrt{2}$. The decay parameters are defined using the helicity amplitudes as

$$\alpha = \frac{|H_+|^2 - |H_-|^2}{|H_+|^2 + |H_-|^2}, \quad \beta = \sqrt{1 - \alpha^2} \sin \Delta, \quad \gamma = \sqrt{1 - \alpha^2} \cos \Delta, \quad (1)$$

where $\Delta = \arg(H_+/H_-)$ is the phase angle difference between the two helicity amplitudes.

The angular distribution is determined by the sum of all possible helicity amplitudes as

$$\frac{d\Gamma}{d\Omega} \propto |M|^2 = \sum_{\lambda_0, \lambda'_0, \lambda_n} \rho_{\lambda_0, \lambda'_0} M_{\lambda_0, \lambda_n} M_{\lambda'_0, \lambda_n}^*, \quad (2)$$

where $\lambda_0^{(\prime)}$ and λ_n run over the helicities of the initial and final baryons, $\rho_{\lambda_0, \lambda'_0}$ is the polarization density matrix of the decaying baryon, and M_{λ_0, λ_n} , $M_{\lambda'_0, \lambda_n}^*$ are the amplitude matrix elements.

For the Λ_b^0 baryon promptly produced in pp collisions, the possible polarization is expected to be perpendicular to the production plane due to parity conservation in strong interactions. Defining the polarization axis as the z -axis, and the magnitude of the polarization as P_z , the polarization density matrix is expressed as

$$\rho = \begin{pmatrix} 1 + P_z & 0 \\ 0 & 1 - P_z \end{pmatrix}. \quad (3)$$

1.1 Angular distribution for $\Lambda_b^0 \rightarrow \Lambda_c^+(\rightarrow pK_S^0)h^-$ decays

For $\Lambda_b^0 \rightarrow \Lambda_c^+(\rightarrow pK_S^0)h^-$ decays, the helicity amplitude is determined as

$$M_{\lambda_b, \lambda_p} = \sum_{\lambda_c} H_{\lambda_c}^b d_{\lambda_b, \lambda_c}^{\frac{1}{2}}(\theta_0) \cdot H_{\lambda_p}^c e^{i\lambda_c \phi_1} d_{\lambda_c, \lambda_p}^{\frac{1}{2}}(\theta_1), \quad (4)$$

where $d_{\lambda, \lambda'}^J(\theta)$ is the Wigner d-matrix, λ_b , λ_c and λ_p refer to the helicities of Λ_b^0 , Λ_c^+ and p baryons, and $H_{\lambda_c}^b$ and $H_{\lambda_p}^c$ are the helicity couplings of Λ_b^0 and Λ_c^+ decays. The total amplitude squared is calculated by

$$|M|^2 \propto \sum_{\lambda_p} [(1 + P_z) \cdot |M_{1/2, \lambda_p}|^2 + (1 - P_z) \cdot |M_{-1/2, \lambda_p}|^2], \quad (5)$$

which leads to

$$\begin{aligned}
\frac{d^3\Gamma}{d\cos\theta_0 d\cos\theta_1 d\phi_1} \propto & 1 + \alpha_{\Lambda_b^0}\alpha_{\Lambda_c^+} \cos\theta_1 \\
& + P_z \cdot (\alpha_{\Lambda_b^0} \cos\theta_0 + \alpha_{\Lambda_c^+} \cos\theta_0 \cos\theta_1 \\
& - \gamma_{\Lambda_b^0}\alpha_{\Lambda_c^+} \sin\theta_0 \sin\theta_1 \cos\phi_1 \\
& + \beta_{\Lambda_b^0}\alpha_{\Lambda_c^+} \sin\theta_0 \sin\theta_1 \sin\phi_1),
\end{aligned} \tag{6}$$

where $\alpha_{\Lambda_b^0}, \beta_{\Lambda_b^0}, \gamma_{\Lambda_b^0}$ are the Λ_b^0 decay parameters defined by H_{\pm}^b , and $\alpha_{\Lambda_c^+}$ is the Λ_c^+ decay parameter related to H_{\pm}^c .

1.2 Angular distribution for $\Lambda_b^0 \rightarrow \Lambda_c^+(\rightarrow \Lambda(\rightarrow p\pi^-)h_1^+)h_2^-$ decays

For $\Lambda_b^0 \rightarrow \Lambda_c^+(\rightarrow \Lambda(\rightarrow p\pi^-)h_1^+)h_2^-$ decays, the relevant angles are $(\theta_0, \theta_1, \phi_1, \theta_2, \phi_2)$, which are defined in Fig. 2. The helicity amplitude is expressed as

$$M_{\lambda_b, \lambda_p} = \sum_{\lambda_c} H_{\lambda_c}^b d_{\lambda_b, \lambda_c}^{\frac{1}{2}}(\theta_0) \cdot H_{\lambda_s}^c e^{i\lambda_c \phi_1} d_{\lambda_c, \lambda_s}^{\frac{1}{2}}(\theta_1) \cdot H_{\lambda_p}^s e^{i\lambda_s \phi_2} d_{\lambda_s, \lambda_p}^{\frac{1}{2}}(\theta_2), \tag{7}$$

where λ_s refers to the helicity of Λ baryons, and $H_{\lambda_s}^c$ and $H_{\lambda_p}^s$ are the helicity couplings of Λ_c^+ and Λ decays. The total amplitude is calculated by Eq. 5, which leads to

$$\begin{aligned}
& \frac{d^5\Gamma}{d\cos\theta_0 d\cos\theta_1 d\phi_1 d\cos\theta_2 d\phi_2} \\
\propto & (1 + \alpha_{\Lambda_b^0}\alpha_{\Lambda_c^+} \cos\theta_1 + \alpha_{\Lambda_c^+}\alpha_{\Lambda} \cos\theta_2 + \alpha_{\Lambda_b^0}\alpha_{\Lambda} \cos\theta_1 \cos\theta_2 \\
& - \alpha_{\Lambda_b^0}\gamma_{\Lambda_c^+}\alpha_{\Lambda} \sin\theta_1 \sin\theta_2 \cos\phi_2 + \alpha_{\Lambda_b^0}\beta_{\Lambda_c^+}\alpha_{\Lambda} \sin\theta_1 \sin\theta_2 \sin\phi_2) \\
& + P_z \cdot (\alpha_{\Lambda_b^0} \cos\theta_0 + \alpha_{\Lambda_c^+} \cos\theta_0 \cos\theta_1 + \alpha_{\Lambda_b^0}\alpha_{\Lambda_c^+}\alpha_{\Lambda} \cos\theta_0 \cos\theta_2 \\
& + \alpha_{\Lambda} \cos\theta_0 \cos\theta_1 \cos\theta_2 - \gamma_{\Lambda_b^0}\alpha_{\Lambda_c^+} \sin\theta_0 \sin\theta_1 \cos\phi_1 + \beta_{\Lambda_b^0}\alpha_{\Lambda_c^+} \sin\theta_0 \sin\theta_1 \sin\phi_1 \\
& - \gamma_{\Lambda_c^+}\alpha_{\Lambda} \cos\theta_0 \sin\theta_1 \sin\theta_2 \cos\phi_2 + \beta_{\Lambda_c^+}\alpha_{\Lambda} \cos\theta_0 \sin\theta_1 \sin\theta_2 \sin\phi_2 \\
& - \gamma_{\Lambda_b^0}\alpha_{\Lambda} \sin\theta_0 \sin\theta_1 \cos\theta_2 \cos\phi_1 + \beta_{\Lambda_b^0}\alpha_{\Lambda} \sin\theta_0 \sin\theta_1 \cos\theta_2 \sin\phi_1 \\
& + \beta_{\Lambda_b^0}\beta_{\Lambda_c^+}\alpha_{\Lambda} \sin\theta_0 \sin\theta_2 \cos\phi_1 \cos\phi_2 + \beta_{\Lambda_b^0}\gamma_{\Lambda_c^+}\alpha_{\Lambda} \sin\theta_0 \sin\theta_2 \cos\phi_1 \sin\phi_2 \\
& + \gamma_{\Lambda_b^0}\beta_{\Lambda_c^+}\alpha_{\Lambda} \sin\theta_0 \sin\theta_2 \sin\phi_1 \cos\phi_2 + \gamma_{\Lambda_b^0}\gamma_{\Lambda_c^+}\alpha_{\Lambda} \sin\theta_0 \sin\theta_2 \sin\phi_1 \sin\phi_2 \\
& - \gamma_{\Lambda_b^0}\gamma_{\Lambda_c^+}\alpha_{\Lambda} \sin\theta_0 \cos\theta_1 \sin\theta_2 \cos\phi_1 \cos\phi_2 \\
& + \gamma_{\Lambda_b^0}\beta_{\Lambda_c^+}\alpha_{\Lambda} \sin\theta_0 \cos\theta_1 \sin\theta_2 \cos\phi_1 \sin\phi_2 \\
& + \beta_{\Lambda_b^0}\gamma_{\Lambda_c^+}\alpha_{\Lambda} \sin\theta_0 \cos\theta_1 \sin\theta_2 \sin\phi_1 \cos\phi_2 \\
& - \beta_{\Lambda_b^0}\beta_{\Lambda_c^+}\alpha_{\Lambda} \sin\theta_0 \cos\theta_1 \sin\theta_2 \sin\phi_1 \sin\phi_2),
\end{aligned} \tag{8}$$

where α_{Λ} is the Λ decay parameter related to H_{\pm}^s .

References

- [1] J. F. Donoghue, X.-G. He, and S. Pakvasa, *Hyperon decays and CP nonconservation*, Phys. Rev. **D34** (1986) 833.
- [2] A. D. Sakharov, *Violation of CP Invariance, C asymmetry, and baryon asymmetry of the universe*, Pisma Zh. Eksp. Teor. Fiz. **5** (1967) 32.
- [3] S.-S. Tang, L.-K. Li, X.-Y. Zhou, and C.-P. Shen, *Recent measurements of decay asymmetry parameter and CP asymmetry for charmed baryon decays at Belle*, Symmetry **15** (2022) 91.
- [4] T. D. Lee and C. N. Yang, *General partial wave analysis of the decay of a hyperon of spin $\frac{1}{2}$* , Phys. Rev. **108** (1957) 1645.
- [5] X. Dai *et al.*, *CP violation in baryon decays at LHCb*, Symmetry **15** (2023) 522, arXiv:2302.00180.
- [6] H.-W. Ke, X.-Q. Li, and Z.-T. Wei, *Diquarks and $\Lambda_b \rightarrow \Lambda_c$ weak decays*, Phys. Rev. **D77** (2008) 014020, arXiv:0710.1927.
- [7] A. K. Leibovich, Z. Ligeti, I. W. Stewart, and M. B. Wise, *Predictions for nonleptonic Λ_b and Θ_b decays*, Phys. Lett. **B586** (2004) 337, arXiv:hep-ph/0312319.
- [8] H.-H. Shih, S.-C. Lee, and H.-n. Li, *Applicability of perturbative QCD to $\Lambda_b \rightarrow \Lambda_c$ decays*, Phys. Rev. **D61** (2000) 114002, arXiv:hep-ph/9906370.
- [9] T. Mannel and W. Roberts, *Nonleptonic Λ_b decays at colliders*, Z. Phys. **C59** (1993) 179.
- [10] C.-Q. Geng, C.-W. Liu, and T.-H. Tsai, *Nonleptonic two-body weak decays of Λ_b in a modified MIT bag model*, Phys. Rev. **D102** (2020) 034033, arXiv:2007.09897.
- [11] J. Zhu, Z.-T. Wei, and H.-W. Ke, *Semileptonic and nonleptonic weak decays of Λ_b^0* , Phys. Rev. **D99** (2019) 054020, arXiv:1803.01297.
- [12] R. Mohanta *et al.*, *Hadronic weak decays of Λ_b baryon in the covariant oscillator quark model*, Progress of Theoretical Physics **101** (1999) 959–969, arXiv:hep-ph/9904324.
- [13] C.-K. Chua, *Color-allowed bottom baryon to S-wave and P-wave charmed baryon nonleptonic decays*, Phys. Rev. **D100** (2019) 034025, arXiv:1905.00153.
- [14] H.-W. Ke, N. Hao, and X.-Q. Li, *Revisiting $\Lambda_b \rightarrow \Lambda_c$ and $\Sigma_b \rightarrow \Sigma_c$ weak decays in the light-front quark model*, Eur. Phys. J. **C79** (2019) 540, arXiv:1904.05705.
- [15] C.-Q. Zhang, J.-M. Li, M.-K. Jia, and Z. Rui, *Nonleptonic two-body decays of $\Lambda_b \rightarrow \Lambda_c \pi$, $\Lambda_c K$ in the perturbative QCD approach*, Phys. Rev. **D105** (2022) 073005, arXiv:2202.09181.
- [16] K. K. Sharma and R. C. Verma, *$SU(3)_{\text{flavor}}$ analysis of two-body weak decays of charmed baryons*, Phys. Rev. **D55** (1997) 7067, arXiv:hep-ph/9704391.

- [17] J. D. Bjorken, *Spin-dependent decays of the Λ_c* , Phys. Rev. **D40** (1989) 1513.
- [18] H.-Y. Cheng and B. Tseng, *Cabibbo-allowed nonleptonic weak decays of charmed baryons*, Phys. Rev. **D48** (1993) 4188, [arXiv:hep-ph/9304286](#).
- [19] Q. P. Xu and A. N. Kamal, *Cabibbo-favored nonleptonic decays of charmed baryons*, Phys. Rev. **D46** (1992) 270.
- [20] T. Uppal, R. C. Verma, and M. P. Khanna, *Constituent quark model analysis of weak mesonic decays of charm baryons*, Phys. Rev. **D49** (1994) 3417.
- [21] P. Żenczykowski, *Nonleptonic charmed-baryon decays: symmetry properties of parity-violating amplitudes*, Phys. Rev. **D50** (1994) 5787.
- [22] J. Zou, F. Xu, G. Meng, and H.-Y. Cheng, *Two-body hadronic weak decays of antitriplet charmed baryons*, Phys. Rev. **D101** (2020) 014011, [arXiv:1910.13626](#).
- [23] J. G. Korner and M. Kramer, *Exclusive nonleptonic charm baryon decays*, Z. Phys. **C55** (1992) 659.
- [24] K. K. Sharma and R. C. Verma, *A Study of weak mesonic decays of Λ_c and Ξ_c baryons on the basis of HQET results*, Eur. Phys. J. **C7** (1999) 217, [arXiv:hep-ph/9803302](#).
- [25] H.-Y. Cheng, X.-W. Kang, and F. Xu, *Singly Cabibbo-suppressed hadronic decays of Λ_c^+* , Phys. Rev. **D97** (2018) 074028, [arXiv:1801.08625](#).
- [26] M. A. Ivanov, J. G. Körner, V. E. Lyubovitskij, and A. G. Rusetsky, *Exclusive nonleptonic decays of bottom and charm baryons in a relativistic three-quark model: Evaluation of nonfactorizing diagrams*, Phys. Rev. **D57** (1998) 5632, [arXiv:hep-ph/9709372](#).
- [27] C. Q. Geng, C.-W. Liu, and T.-H. Tsai, *Asymmetries of anti-triplet charmed baryon decays*, Phys. Lett. **B794** (2019) 19, [arXiv:1902.06189](#).
- [28] Particle Data Group, S. Navas *et al.*, *Review of particle physics*, Phys. Rev. D **110** (2024) 030001.
- [29] BESIII collaboration, M. Ablikim *et al.*, *Polarization and entanglement in baryon-antibaryon pair production in electron-positron annihilation*, Nature Phys. **15** (2019) 631, [arXiv:1808.08917](#).
- [30] BESIII collaboration, M. Ablikim *et al.*, *Precise measurements of decay parameters and CP asymmetry with entangled $\Lambda - \bar{\Lambda}$ pairs*, Phys. Rev. Lett. **129** (2022) 131801, [arXiv:2204.11058](#).
- [31] D. G. Ireland *et al.*, *Kaon photoproduction and the Λ decay parameter α_-* , Phys. Rev. Lett. **123** (2019) 182301, [arXiv:1904.07616](#).
- [32] Particle Data Group, M. Tanabashi *et al.*, *Review of particle physics*, Phys. Rev. **D98** (2018) 030001.

- [33] FOCUS collaboration, J. M. Link *et al.*, *Study of the decay asymmetry parameter and CP violation parameter in the $\Lambda_c^+ \rightarrow \Lambda\pi^+$ decay*, Phys. Lett. **B634** (2006) 165, [arXiv:hep-ex/0509042](#).
- [34] BESIII collaboration, M. Ablikim *et al.*, *Measurements of weak decay asymmetries of $\Lambda_c^+ \rightarrow pK_S^0$, $\Lambda\pi^+$, $\Sigma^+\pi^0$, and $\Sigma^0\pi^+$* , Phys. Rev. **D100** (2019) 072004, [arXiv:1905.04707](#).
- [35] Belle collaboration, L. K. Li *et al.*, *Search for CP violation and measurement of branching fractions and decay asymmetry parameters for $\Lambda_c^+ \rightarrow \Lambda h^+$ and $\Lambda_c^+ \rightarrow \Sigma^0 h^+$ ($h = K, \pi$)*, Sci. Bull. **68** (2023) 583, [arXiv:2208.08695](#).
- [36] BESIII collaboration, M. Ablikim *et al.*, *First measurement of the decay asymmetry in the pure W-boson-exchange decay $\Lambda_c^+ \rightarrow \Xi^0 K^+$* , Phys. Rev. Lett. **132** (2024) 031801, [arXiv:2309.02774](#).
- [37] LHCb collaboration, R. Aaij *et al.*, *Measurements of the $\Lambda_b^0 \rightarrow J/\psi\Lambda$ decay amplitudes and the Λ_b^0 polarisation in pp collisions at $\sqrt{s} = 7$ TeV*, Phys. Lett. **B724** (2013) 27, [arXiv:1302.5578](#).
- [38] LHCb collaboration, R. Aaij *et al.*, *Measurement of the $\Lambda_b^0 \rightarrow J/\psi\Lambda$ angular distribution and the Λ polarisation in pp collisions*, JHEP **06** (2020) 110, [arXiv:2004.10563](#).
- [39] ATLAS collaboration, G. Aad *et al.*, *Measurement of the parity-violating asymmetry parameter α_b and the helicity amplitudes for the decay $\Lambda_b^0 \rightarrow J/\psi + \Lambda^0$ with the ATLAS detector*, Phys. Rev. **D89** (2014) 092009, [arXiv:1404.1071](#).
- [40] CMS collaboration, A. M. Sirunyan *et al.*, *Measurement of the Λ_b polarization and angular parameters in $\Lambda_b \rightarrow J/\psi\Lambda$ decays from pp collisions at $\sqrt{s} = 7$ and 8 TeV*, Phys. Rev. **D97** (2018) 072010, [arXiv:1802.04867](#).
- [41] LHCb collaboration, R. Aaij *et al.*, *Measurement of the photon polarization in $\Lambda_b^0 \rightarrow \Lambda\gamma$ decays*, Phys. Rev. **D105** (2022) 051104, [arXiv:2111.10194](#).
- [42] LHCb collaboration, A. A. Alves Jr. *et al.*, *The LHCb detector at the LHC*, JINST **3** (2008) S08005.
- [43] LHCb collaboration, R. Aaij *et al.*, *LHCb detector performance*, Int. J. Mod. Phys. **A30** (2015) 1530022, [arXiv:1412.6352](#).
- [44] R. Aaij *et al.*, *The LHCb trigger and its performance in 2011*, JINST **8** (2013) P04022, [arXiv:1211.3055](#).
- [45] LHCb collaboration, *LHCb Trigger and Online Upgrade Technical Design Report*, CERN-LHCC-2014-016, 2014.
- [46] T. Likhomanenko *et al.*, *LHCb topological trigger reoptimization*, J. Phys. Conf. Ser. **664** (2015) 082025, [arXiv:1510.00572](#).
- [47] V. V. Gligorov and M. Williams, *Efficient, reliable and fast high-level triggering using a bonsai boosted decision tree*, JINST **8** (2013) P02013, [arXiv:1210.6861](#).

- [48] R. Aaij *et al.*, *Design and performance of the LHCb trigger and full real-time reconstruction in Run 2 of the LHC*, JINST **14** (2019) P04013, [arXiv:1812.10790](#).
- [49] T. Sjöstrand, S. Mrenna, and P. Skands, *A brief introduction to PYTHIA 8.1*, Comput. Phys. Commun. **178** (2008) 852, [arXiv:0710.3820](#); T. Sjöstrand, S. Mrenna, and P. Skands, *PYTHIA 6.4 physics and manual*, JHEP **05** (2006) 026, [arXiv:hep-ph/0603175](#).
- [50] I. Belyaev *et al.*, *Handling of the generation of primary events in Gauss, the LHCb simulation framework*, J. Phys. Conf. Ser. **331** (2011) 032047.
- [51] D. J. Lange, *The EvtGen particle decay simulation package*, Nucl. Instrum. Meth. **A462** (2001) 152.
- [52] N. Davidson, T. Przedzinski, and Z. Was, *PHOTOS interface in C++: Technical and physics documentation*, Comp. Phys. Comm. **199** (2016) 86, [arXiv:1011.0937](#).
- [53] Geant4 collaboration, J. Allison *et al.*, *Geant4 developments and applications*, IEEE Trans. Nucl. Sci. **53** (2006) 270; Geant4 collaboration, S. Agostinelli *et al.*, *Geant4: A simulation toolkit*, Nucl. Instrum. Meth. **A506** (2003) 250.
- [54] M. Clemencic *et al.*, *The LHCb simulation application, Gauss: Design, evolution and experience*, J. Phys. Conf. Ser. **331** (2011) 032023.
- [55] A. Hoecker *et al.*, *TMVA 4 — Toolkit for Multivariate Data Analysis with ROOT. Users Guide.*, [arXiv:physics/0703039](#).
- [56] W. D. Hulsbergen, *Decay chain fitting with a Kalman filter*, Nucl. Instrum. Meth. **A552** (2005) 566, [arXiv:physics/0503191](#).
- [57] D. Martínez Santos and F. Dupertuis, *Mass distributions marginalized over per-event errors*, Nucl. Instrum. Meth. **A764** (2014) 150, [arXiv:1312.5000](#).
- [58] M. Pivk and F. R. Le Diberder, *sPlot: A statistical tool to unfold data distributions*, Nucl. Instrum. Meth. **A555** (2005) 356, [arXiv:physics/0402083](#).
- [59] M. Jacob and G. C. Wick, *On the general theory of collisions for particles with spin*, Annals Phys. **7** (1959) 404.
- [60] C. Langenbruch, *Parameter uncertainties in weighted unbinned maximum likelihood fits*, Eur. Phys. J. **C82** (2022) 393, [arXiv:1911.01303](#).
- [61] R. E. Caflisch, *Monte Carlo and quasi-Monte Carlo methods*, Acta Numerica **7** (1998) 1.
- [62] See Supplemental Material for details.
- [63] L. Anderlini *et al.*, *The PIDCalib package*, LHCb-PUB-2016-021, 2016.
- [64] R. Aaij *et al.*, *Selection and processing of calibration samples to measure the particle identification performance of the LHCb experiment in Run 2*, Eur. Phys. J. Tech. Instr. **6** (2019) 1, [arXiv:1803.00824](#).

- [65] B. Efron, *Bootstrap methods: Another look at the jackknife*, Ann. Statist. **7** (1979) 1.
- [66] LHCb collaboration, R. Aaij *et al.*, *Measurement of B^0 , B_s^0 , B^+ and Λ_b^0 production asymmetries in 7 and 8 TeV proton-proton collisions*, Phys. Lett. **B774** (2017) 139, [arXiv:1703.08464](#).
- [67] LHCb collaboration, R. Aaij *et al.*, *Observation of a $\Lambda_b^0 - \bar{\Lambda}_b^0$ production asymmetry in proton-proton collisions at $\sqrt{s} = 7$ and 8 TeV*, JHEP **10** (2021) 060, [arXiv:2107.09593](#).
- [68] LHCb collaboration, R. Aaij *et al.*, *Measurement of the time-integrated CP asymmetry in $D^0 \rightarrow K^- K^+$ decays*, Phys. Rev. Lett. **131** (2023) 091802, [arXiv:2209.03179](#).
- [69] LHCb collaboration, R. Aaij *et al.*, *Search for CP violation in $\Lambda_b^0 \rightarrow pK^-$ and $\Lambda_b^0 \rightarrow p\pi^-$ decays*, Phys. Lett. **B784** (2018) 101, [arXiv:1807.06544](#).
- [70] LHCb collaboration, R. Aaij *et al.*, *Search for CP violation using triple product asymmetries in $\Lambda_b^0 \rightarrow pK^- \pi^+ \pi^-$, $\Lambda_b^0 \rightarrow pK^- K^+ K^-$, and $\Xi_b^0 \rightarrow pK^- K^- \pi^+$ decays*, JHEP **08** (2018) 039, [arXiv:1805.03941](#).
- [71] F. J. Botella *et al.*, *On the search for the electric dipole moment of strange and charm baryons at LHC*, Eur. Phys. J. **C77** (2017) 181, [arXiv:1612.06769](#).
- [72] H.-Y. Cheng, *Nonleptonic weak decays of bottom baryons*, Phys. Rev. **D56** (1997) 2799, [arXiv:hep-ph/9612223](#).
- [73] H. Zhong, F. Xu, and H.-Y. Cheng, *Analysis of hadronic weak decays of charmed baryons in the topological diagrammatic approach*, Phys. Rev. **D109** (2024) 114027, [arXiv:2404.01350](#).

2 PRL Justification

This letter presents a comprehensive study of parity and charge-parity (CP) violation in decays of bottom, charm and strange baryons using the angular analysis method initially proposed by T.D. Lee and C.N. Yang. The major results include the first measurement of the decay parameters for $\Lambda_b^0 \rightarrow \Lambda_c^+ h^+$ ($h = K, \pi$) decays, the most precise determinations of the decay parameters α, β, γ for $\Lambda_c^+ \rightarrow \Lambda^0 h^+$ ($h = K, \pi$) decays, α for $\Lambda_c^+ \rightarrow p K_S^0$ decay and the associated CP asymmetries, as well as an independent confirmation of the decay parameter $\alpha(\Lambda^0 \rightarrow p\pi^-)$ measured by the BESIII experiment, which was significantly higher than the previous world average. These results support the factorization hypothesis in theoretical calculations of beauty baryon hadronic decays, and indicate the importance of nonfactorizable contributions in hadronic decays of charm baryons. This is the first study of its kind at LHCb and at a hadron collider, demonstrating LHCb's great potential to study CP violation in baryon decays via the angular analysis approach.

2.1 Word count

- Text (captions included): 3022
- Math display: 128
- Tables: 188.5
- Figures: 431
- All: 3770

Supplemental material

1 Summary of systematic uncertainties

The various sources of systematic uncertainties on the decay parameter measurements, including fit procedure, mass fit model, PID calibration, limited size of simulation samples, production and detection asymmetries and Λ_b^0 polarization, are summarized in Table S1, Table S2 and Table S3. The total systematic uncertainties correspond to the sum in quadrature of all sources.

Table S1: Systematic uncertainties ($\times 10^{-3}$) on α parameters of different decays. For each cell, the four values are for baryon decays (α), antibaryon decays ($\bar{\alpha}$), their averages ($\langle\alpha\rangle$) and asymmetries (A_α).

Sources	$\Lambda_b^0 \rightarrow \Lambda_c^+ \pi^-$	$\Lambda_b^0 \rightarrow \Lambda_c^+ K^-$	$\Lambda_c^+ \rightarrow \Lambda \pi^+$	$\Lambda_c^+ \rightarrow \Lambda K^+$	$\Lambda_c^+ \rightarrow p K_S^0$	$\Lambda \rightarrow p \pi^-$
Fit	0.1/0.7/0.5/0.3	2.4/6.6/1.5/4.6	0.9/0.6/0.1/0.8	3.5/0.9/1.9/2.0	0.1/0.3/0.0/0.2	0.2/0.3/0.1/0.1
Mass	1.1/0.9/0.9/0.3	4.0/6.0/6.2/1.3	0.5/0.6/0.5/0.1	23.3/6.7/13.8/22.7	1.7/1.6/1.7/0.3	1.4/1.7/1.2/0.3
PID	0.4/0.3/0.3/0.0	3.6/3.0/3.6/0.6	0.5/0.5/0.1/0.1	4.2/3.9/4.7/0.9	0.8/0.8/0.5/0.1	0.9/0.8/0.7/0.1
MC	2.6/2.3/2.5/0.2	12.0/9.2/10.6/1.9	2.7/2.6/2.6/0.2	14.4/15.2/14.7/4.9	4.4/4.3/4.4/0.2	5.5/5.1/5.3/0.6
Asym.	1.0/1.0/0.2/1.0	0.7/1.0/0.2/0.9	1.2/1.0/0.0/1.4	1.2/1.9/0.6/0.3	5.0/5.4/0.4/6.9	4.0/4.0/0.1/5.5
Polar.	0.8/0.6/4.4/4.5	4.3/0.8/7.6/2.7	1.9/1.0/1.2/1.5	4.7/1.4/1.4/1.1	4.6/0.9/3.0/4.4	4.6/0.9/2.8/3.5
Total	3.1/2.9/5.2/4.7	14.1/13.3/15.0/5.9	3.7/2.9/2.9/2.2	28.4/17.3/20.8/23.4	8.7/7.2/5.6/8.2	8.7/6.8/6.2/6.6

Table S2: Systematic uncertainties ($\times 10^{-3}$) on the decay parameters β and γ , the phase difference Δ , the CP asymmetry R_β and the CP average R'_β for $\Lambda_c^+ \rightarrow \Lambda \pi^+$ decay.

Sources	$\beta/\bar{\beta}/R_\beta/R'_\beta$	$\gamma/\bar{\gamma}$	$\Delta/\bar{\Delta}$ (rad)
Fit	0.2/0.1/0.2/0.1	0.6/1.1	0.1/2.0
Mass	1.3/1.3/0.5/0.8	0.5/1.0	1.1/1.1
PID	1.1/1.1/0.1/0.9	0.8/0.7	1.2/1.2
MC	6.7/8.8/0.5/8.5	5.4/6.6	11.9/11.0
Asym.	3.5/4.4/5.2/0.5	1.1/1.7	5.8/7.1
Polar.	0.2/0.3/0.9/1.4	0.7/1.1	1.1/0.2
Total	7.7/10.0/5.3/8.7	5.7/7.1	13.4/13.4

Table S3: Systematic uncertainties ($\times 10^{-3}$) on the decay parameters β and γ , the phase difference Δ , the CP asymmetry R_β and the CP average R'_β for $\Lambda_c^+ \rightarrow \Lambda K^+$ decay.

Sources	$\beta/\bar{\beta}/R_\beta/R'_\beta$	$\gamma/\bar{\gamma}$	$\Delta/\bar{\Delta}$ (rad)
Fit	12.0/2.6/9.5/13.2	8.0/1.4	7.0/1.3
Mass	12.2/6.2/13.1/25.4	15.9/3.3	9.7/5.9
PID	6.9/4.2/2.7/15.2	1.6/1.6	11.1/7.7
MC	32.5/26.4/9.2/54.9	16.0/12.7	37.9/27.7
Asym.	1.4/1.8/3.1/1.1	1.4/0.4	1.8/2.9
Polar.	0.4/2.4/0.1/0.2	0.6/1.1	3.2/4.7
Total	37.4/27.8/19.1/64.1	24.0/13.4	41.5/29.9

2 Projections of angular distributions

Projections of angular distributions and fit results for various decays studied in the Letter are shown in Figs. S1, S2, S3, S4 and S5.

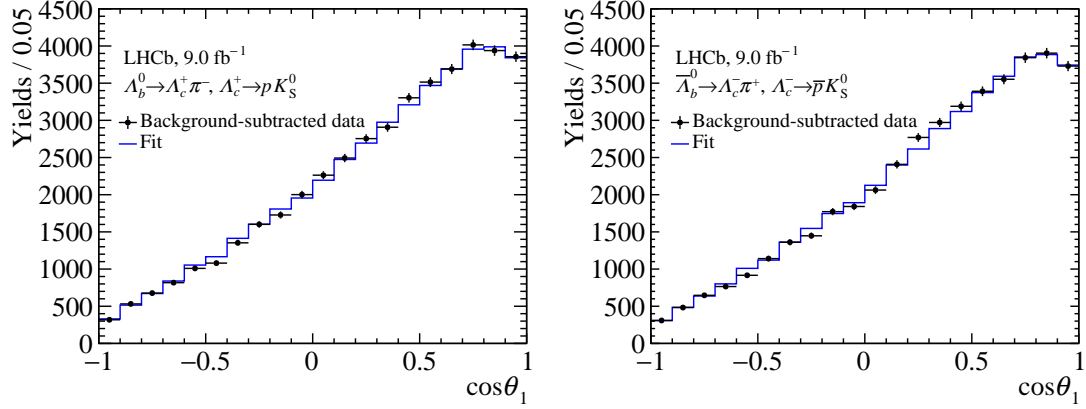


Figure S1: Distributions of $\cos\theta_1$ for (left) the $\Lambda_b^0 \rightarrow \Lambda_c^+(\rightarrow p K_S^0)\pi^-$ decay and (right) its charge-conjugate decay.

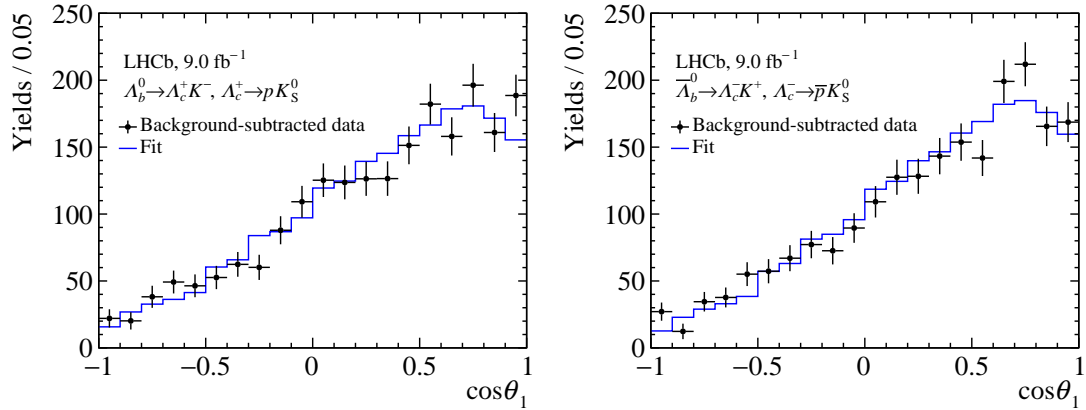


Figure S2: Distributions of $\cos\theta_1$ for (left) the $\Lambda_b^0 \rightarrow \Lambda_c^+(\rightarrow p K_S^0)K^-$ decay and (right) its charge-conjugate decay.

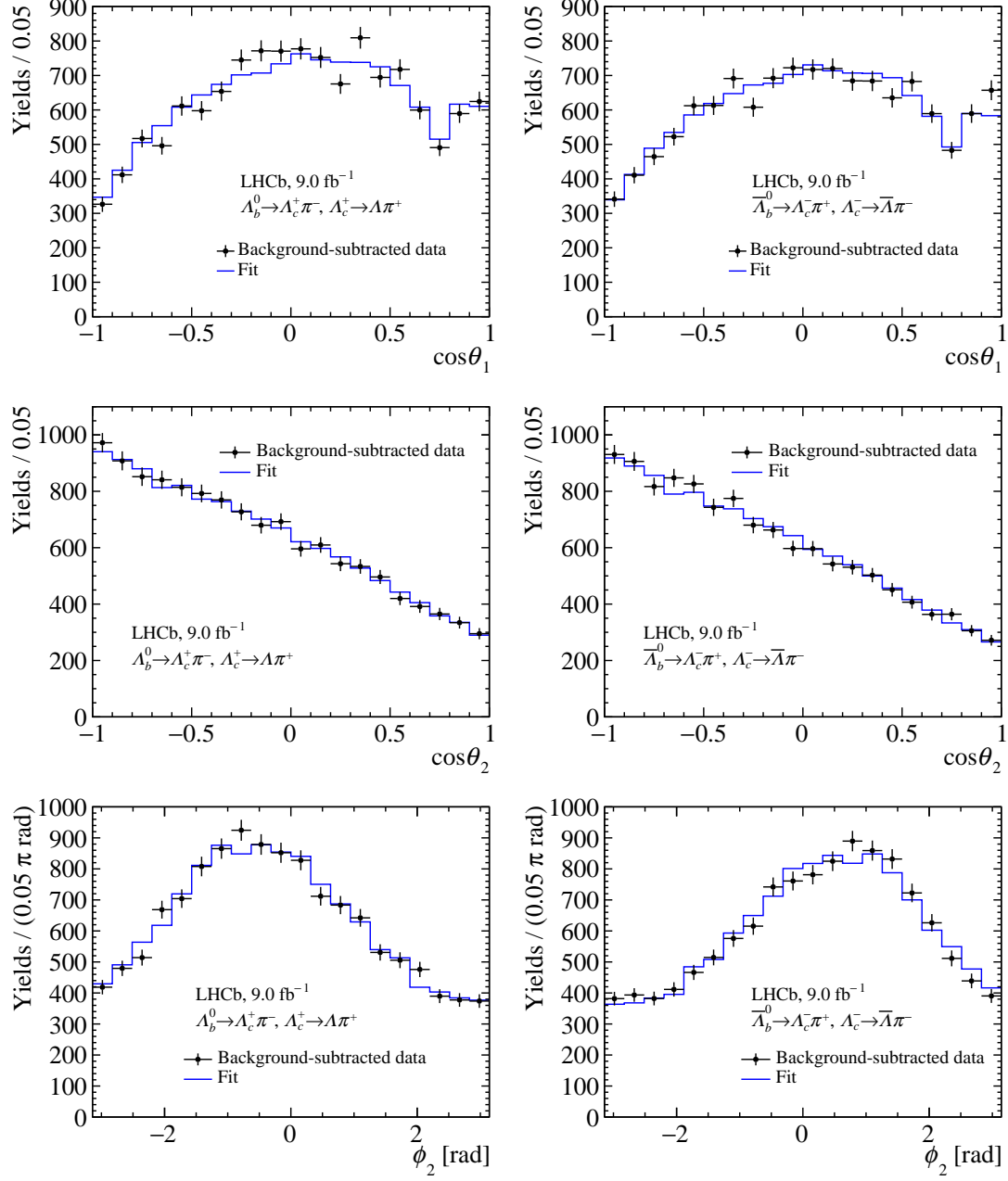


Figure S3: Distributions of (top) $\cos\theta_1$, (middle) $\cos\theta_2$ and (bottom) ϕ_2 for (left) the $\Lambda_b^0 \rightarrow \Lambda_c^+ (\rightarrow \Lambda \pi^+) \pi^-$ decay and (right) its charge-conjugate decay.

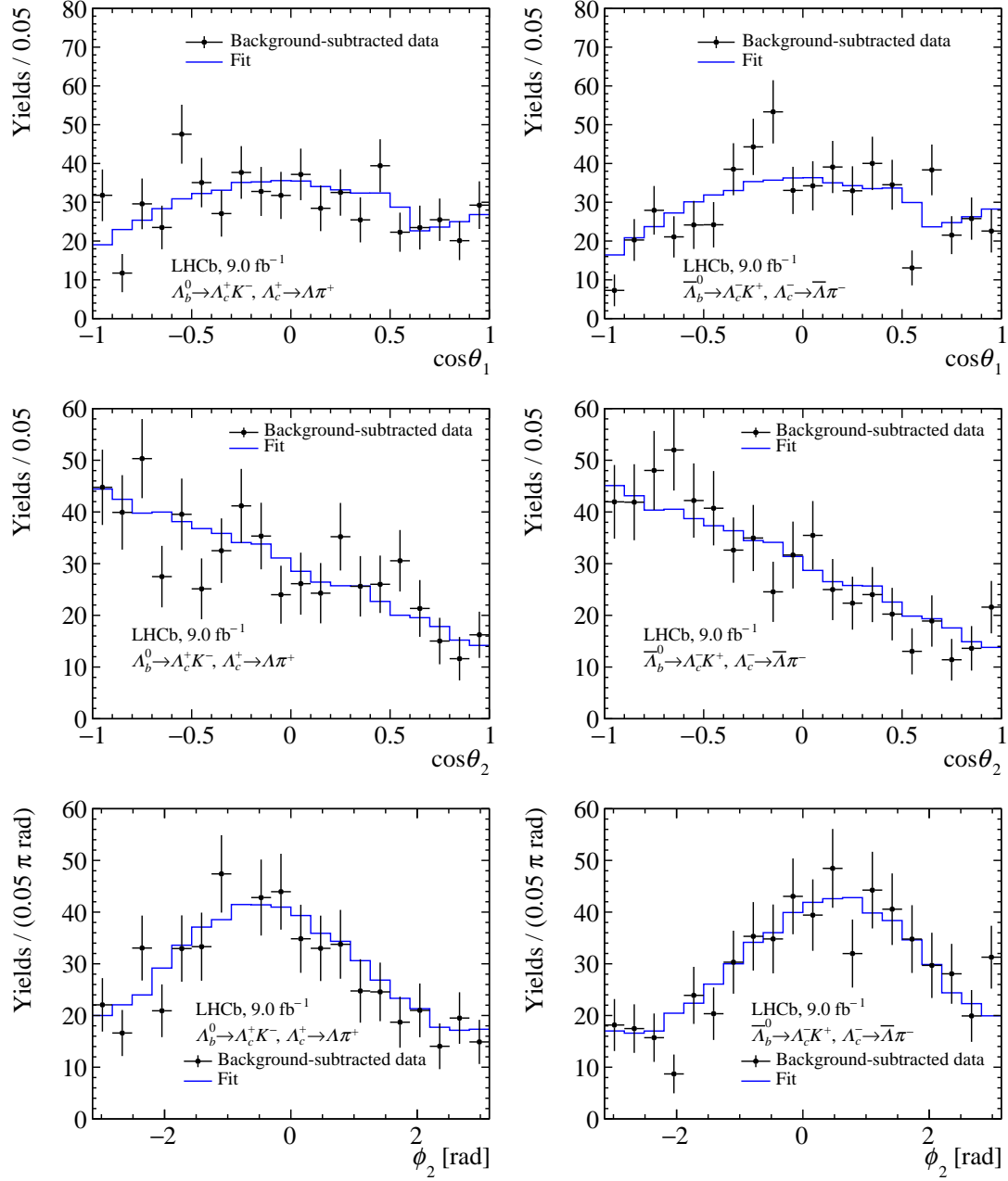


Figure S4: Distributions of (top) $\cos\theta_1$, (middle) $\cos\theta_2$ and (bottom) ϕ_2 for (left) the $\Lambda_b^0 \rightarrow \Lambda_c^+(\rightarrow \Lambda\pi^+)K^-$ decay and (right) its charge-conjugate decay.

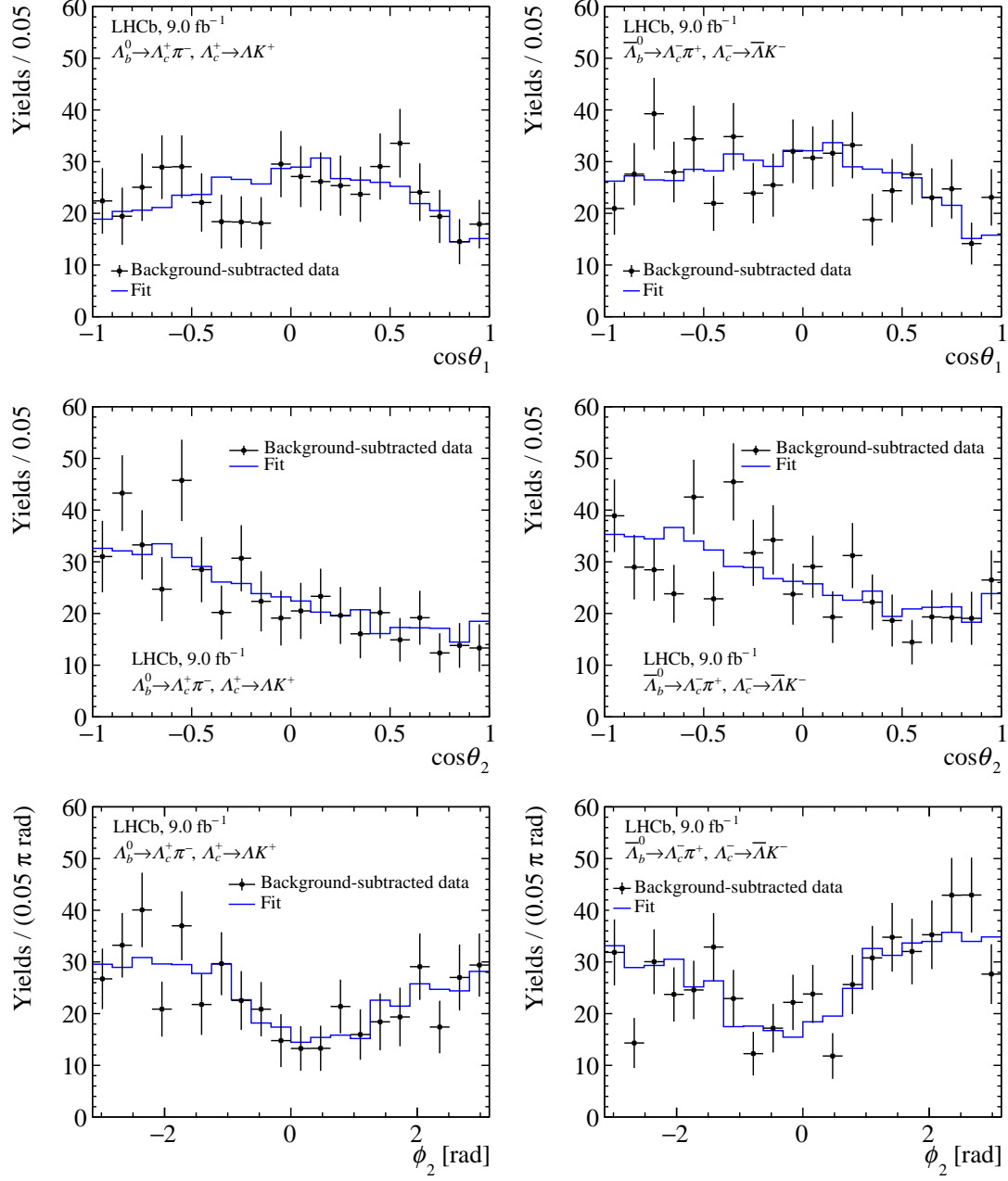


Figure S5: Distributions of (top) $\cos\theta_1$, (middle) $\cos\theta_2$ and (bottom) ϕ_2 for (left) the $\Lambda_b^0 \rightarrow \Lambda_c^+(\rightarrow \Lambda K^+)\pi^-$ decay and (right) its charge-conjugate decay.

3 Correlation matrices for parameters

Correlation matrices between decay parameters without accounting for systematic uncertainties are provided in Tables S4-S7. The correlation matrix between CP -related parameters is provided in Table S8.

Table S4: Correlation matrix of decay parameters for baryon decays using α, Δ as fit parameters.

	$\alpha_{\Lambda_b^0}^{\Lambda_c^+ \pi^-}$	$\alpha_{\Lambda_b^0}^{\Lambda_c^+ K^-}$	$\alpha_{\Lambda_c^+}^{\Lambda \pi^+}$	$\alpha_{\Lambda_c^+}^{\Lambda K^+}$	$\Delta_{\Lambda_c^+}^{\Lambda \pi^+}$	$\Delta_{\Lambda_c^+}^{\Lambda K^+}$	$\alpha_{\Lambda}^{p\pi^-}$	$\alpha_{\Lambda_c^+}^{pK_S^0}$
$\alpha_{\Lambda_b^0}^{\Lambda_c^+ \pi^-}$	1.000	0.154	-0.345	-0.079	-0.004	0.005	0.424	-0.671
$\alpha_{\Lambda_b^0}^{\Lambda_c^+ K^-}$		1.000	-0.106	-0.013	0.007	0.001	0.091	-0.201
$\alpha_{\Lambda_c^+}^{\Lambda \pi^+}$			1.000	0.027	0.005	-0.002	-0.128	0.237
$\alpha_c^{\Lambda K}$				1.000	-0.068	-0.049	-0.067	0.053
$\Delta_{\Lambda_c^+}^{\Lambda \pi^+}$					1.000	-0.066	0.007	-0.003
$\Delta_{\Lambda_c^+}^{\Lambda K^+}$						1.000	0.003	-0.003
$\alpha_{\Lambda}^{p\pi^-}$							1.000	-0.287
$\alpha_{\Lambda_c^+}^{pK_S^0}$								1.000

Table S5: Correlation matrix of decay parameters for antibaryon decays using α, Δ as fit parameters.

	$\bar{\alpha}_{\Lambda_b^0}^{\Lambda_c^- \pi^+}$	$\bar{\alpha}_{\Lambda_b^0}^{\Lambda_c^- K^+}$	$\bar{\alpha}_{\Lambda_c^-}^{\bar{\Lambda} \pi^-}$	$\bar{\alpha}_{\Lambda_c^-}^{\bar{\Lambda} K^-}$	$\bar{\Delta}_{\Lambda_c^-}^{\bar{\Lambda} \pi^-}$	$\bar{\Delta}_{\Lambda_c^-}^{\bar{\Lambda} K^-}$	$\bar{\alpha}_{\bar{\Lambda}}^{\bar{p}\pi^+}$	$\bar{\alpha}_{\Lambda_c^-}^{\bar{p}K_S^0}$
$\bar{\alpha}_{\Lambda_b^0}^{\Lambda_c^- \pi^+}$	1.000	0.164	-0.306	-0.035	0.046	-0.002	0.380	-0.660
$\bar{\alpha}_{\Lambda_b^0}^{\Lambda_c^- K^+}$		1.000	-0.044	-0.006	0.021	-0.001	0.113	-0.230
$\bar{\alpha}_{\Lambda_c^-}^{\bar{\Lambda} \pi^-}$			1.000	0.011	-0.021	0.001	-0.115	0.201
$\bar{\alpha}_{\Lambda_c^-}^{\bar{\Lambda} K^-}$				1.000	0.013	-0.017	-0.052	0.023
$\bar{\Delta}_{\Lambda_c^-}^{\bar{\Lambda} \pi^-}$					1.000	0.001	-0.052	-0.032
$\bar{\Delta}_{\Lambda_c^-}^{\bar{\Lambda} K^-}$						1.000	0.009	0.001
$\bar{\alpha}_{\bar{\Lambda}}^{\bar{p}\pi^+}$							1.000	-0.257
$\bar{\alpha}_{\Lambda_c^-}^{\bar{p}K_S^0}$								1.000

Table S6: Correlation matrix of decay parameters for baryon decays using β, γ as fit parameters, with constraint $\alpha^2 + \beta^2 + \gamma^2 = 1$ imposed.
















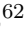

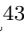









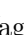















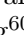
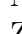



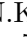

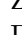



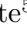
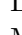
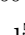



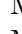
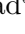
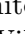


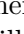
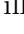

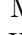




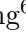






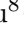



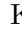


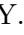

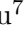



















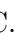



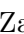



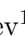
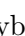



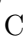









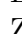
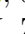
	$\alpha_{\Lambda_b^0}^{A_c^+ \pi^-}$	$\alpha_{\Lambda_b^0}^{A_c^+ K^-}$	$\beta_{\Lambda_c^+}^{A \pi^+}$	$\beta_{\Lambda_c^+}^{A K^+}$	$\gamma_{\Lambda_c^+}^{A \pi^+}$	$\gamma_{\Lambda_c^+}^{A K^+}$	$\alpha_{\Lambda}^{p \pi^-}$	$\alpha_{\Lambda_c^+}^{p K_S^0}$
$\alpha_{\Lambda_b^0}^{A_c^+ \pi^-}$	1.000	0.154	-0.120	-0.016	-0.189	0.040	0.424	-0.671
$\alpha_{\Lambda_b^0}^{A_c^+ K^-}$		1.000	-0.029	-0.003	-0.065	0.006	0.091	-0.201
$\beta_{\Lambda_c^+}^{A \pi^+}$			1.000	0.002	-0.592	-0.005	-0.106	0.082
$\beta_{\Lambda_c^+}^{A K^+}$				1.000	0.002	0.746	-0.014	0.011
$\gamma_{\Lambda_c^+}^{A \pi^+}$					1.000	-0.007	-0.016	0.130
$\gamma_{\Lambda_c^+}^{A K^+}$						1.000	0.021	-0.027
$\alpha_{\Lambda}^{p \pi^-}$							1.000	-0.287
$\alpha_{\Lambda_c^+}^{p K_S^0}$								1.000

Table S7: Correlation matrix of decay parameters for antibaryon decays using β, γ as fit parameters, with constraint $\alpha^2 + \beta^2 + \gamma^2 = 1$ imposed.

	$\bar{\alpha}_{\Lambda_b^0}^{A_c^- \pi^+}$	$\bar{\alpha}_{\Lambda_b^0}^{A_c^- K^+}$	$\bar{\beta}_{\Lambda_c^-}^{\bar{A} \pi^-}$	$\bar{\beta}_{\Lambda_c^-}^{\bar{A} K^-}$	$\bar{\gamma}_{\Lambda_c^-}^{\bar{A} \pi^-}$	$\bar{\gamma}_{\Lambda_c^-}^{\bar{A} K^-}$	$\bar{\alpha}_{\bar{\Lambda}}^{\bar{p} \pi^+}$	$\bar{\alpha}_{\Lambda_c^-}^{\bar{p} K_S^0}$
$\bar{\alpha}_{\Lambda_b^0}^{A_c^- \pi^+}$	1.000	-0.164	0.072	0.002	-0.204	-0.021	-0.380	0.660
$\bar{\alpha}_{\Lambda_b^0}^{A_c^- K^+}$		1.000	0.003	0.000	0.042	0.021	0.113	-0.230
$\bar{\beta}_{\Lambda_c^-}^{\bar{A} \pi^-}$			1.000	-0.000	0.579	-0.002	-0.090	0.046
$\bar{\beta}_{\Lambda_c^-}^{\bar{A} K^-}$				1.000	-0.001	0.751	-0.014	0.011
$\bar{\gamma}_{\Lambda_c^-}^{\bar{A} \pi^-}$					1.000	-0.001	-0.136	0.017
$\bar{\gamma}_{\Lambda_c^-}^{\bar{A} K^-}$						1.000	0.021	-0.257
$\bar{\alpha}_{\bar{\Lambda}}^{\bar{p} \pi^+}$							1.000	-0.257
$\bar{\alpha}_{\Lambda_c^-}^{\bar{p} K_S^0}$								1.000

Table S8: Correlation matrix for the CP -related parameters.

	$\langle \alpha_{A_b^0}^{A_c^+ \pi^-} \rangle$	$A_{\alpha_{A_b^0}}^{A_c^+ \pi^-}$	$\langle \alpha_{A_b^0}^{A_c^+ K^-} \rangle$	$A_{\alpha_{A_b^0}}^{A_c^+ K^-}$	$\langle \alpha_{A_c^+}^{A \pi^+} \rangle$	$A_{\alpha_{A_c^+}}^{A \pi^+}$	$R_{\beta_{A_c^+}}^{A \pi^+}$	$R_{\beta_{A_c^+}}^{A \pi^+}$	$\langle \alpha_{A_c^+}^{AK^+} \rangle$	$A_{\alpha_{A_c^+}}^{AK^+}$	$R_{\beta_{A_c^+}}^{AK^+}$	$R_{\beta_{A_c^+}}^{AK^+}$	$\langle \alpha_{A_c^+}^{pK_S^0} \rangle$	$A_{\alpha_{A_c^+}}^{pK_S^0}$	$\langle \alpha_{A_c^+}^{p\pi^-} \rangle$	$A_{\alpha_{A_c^+}}^{p\pi^-}$
$\langle \alpha_{A_b^0}^{A_c^+ \pi^-} \rangle$	1.000	-0.033	0.159	-0.013	-0.326	0.030	0.026	-0.153	-0.057	0.018	0.009	-0.025	-0.668	0.025	0.405	0.044
$A_{\alpha_{A_b^0}}^{A_c^+ \pi^-}$	1.000	1.000	-0.007	0.158	-0.026	-0.326	-0.097	-0.031	-0.022	-0.054	-0.010	-0.014	-0.011	-0.666	-0.032	-0.404
$\langle \alpha_{A_b^0}^{A_c^+ K^-} \rangle$	1.000	1.000	1.000	-0.164	-0.077	0.036	-0.017	-0.029	-0.004	-0.009	-0.002	-0.004	-0.214	0.001	-0.101	-0.001
$A_{\alpha_{A_b^0}}^{A_c^+ K^-}$	1.000	1.000	1.000	-0.039	-0.078	-0.078	-0.015	-0.024	-0.004	-0.009	-0.002	-0.003	-0.005	-0.213	-0.000	-0.100
$\langle \alpha_{A_c^+}^{A \pi^+} \rangle$	1.000	1.000	1.000	-0.023	-0.020	-0.531	0.019	-0.007	-0.003	-0.005	0.220	-0.022	-0.122	-0.012	-0.122	-0.012
$A_{\alpha_{A_c^+}}^{A \pi^+}$	1.000	1.000	1.000	0.367	0.005	0.018	0.008	0.003	0.005	0.019	0.219	0.009	0.122	0.122	0.009	0.122
$R_{\beta_{A_c^+}}^{A \pi^+}$	1.000	1.000	1.000	0.043	-0.010	0.004	0.002	0.004	0.002	0.004	-0.102	-0.015	0.010	0.010	0.065	0.010
$R_{\beta_{A_c^+}}^{A \pi^+}$	1.000	1.000	1.000	0.043	-0.010	0.004	0.002	0.003	0.003	0.003	-0.018	0.023	0.065	0.015	0.065	0.015
$\langle \alpha_{A_c^+}^{AK^+} \rangle$	1.000	1.000	1.000	0.095	-0.077	-0.428	0.038	-0.015	-0.033	-0.017	0.032	0.032	0.010	0.010	0.010	0.010
$A_{\alpha_{A_c^+}}^{AK^+}$	1.000	1.000	1.000	0.095	-0.077	-0.428	0.038	-0.015	-0.033	-0.017	0.032	0.032	0.010	0.010	0.010	0.010
$R_{\beta_{A_c^+}}^{AK^+}$	1.000	1.000	1.000	0.095	-0.077	-0.428	0.038	-0.015	-0.033	-0.017	0.032	0.032	0.010	0.010	0.010	0.010
$\langle \alpha_{A_c^+}^{pK_S^0} \rangle$	1.000	1.000	1.000	0.095	-0.077	-0.428	0.038	-0.015	-0.033	-0.017	0.032	0.032	0.010	0.010	0.010	0.010
$A_{\alpha_{A_c^+}}^{pK_S^0}$	1.000	1.000	1.000	0.095	-0.077	-0.428	0.038	-0.015	-0.033	-0.017	0.032	0.032	0.010	0.010	0.010	0.010
$\langle \alpha_{A_c^+}^{p\pi^-} \rangle$	1.000	1.000	1.000	0.095	-0.077	-0.428	0.038	-0.015	-0.033	-0.017	0.032	0.032	0.010	0.010	0.010	0.010
$A_{\alpha_{A_c^+}}^{p\pi^-}$	1.000	1.000	1.000	0.095	-0.077	-0.428	0.038	-0.015	-0.033	-0.017	0.032	0.032	0.010	0.010	0.010	0.010

N. Valls Canudas⁴⁷ , H. Van Hecke⁶⁶ , E. van Herwijnen⁶⁰ , C.B. Van Hulse^{45,x} ,
R. Van Laak⁴⁸ , M. van Veghel³⁶ , G. Vasquez⁴⁹ , R. Vazquez Gomez⁴⁴ ,
P. Vazquez Regueiro⁴⁵ , C. Vázquez Sierra⁴⁵ , S. Vecchi²⁴ , J.J. Velthuis⁵³ ,
M. Veltri^{25,w} , A. Venkateswaran⁴⁸ , M. Vesterinen⁵⁵ , D. Vico Benet⁶² ,
M. Vieites Diaz⁴⁷ , X. Vilasis-Cardona⁴³ , E. Vilella Figueras⁵⁹ , A. Villa²³ ,
P. Vincent¹⁵ , F.C. Volle⁵² , D. vom Bruch¹² , N. Voropaev⁴² , K. Vos⁷⁷ ,
G. Vouters^{10,47} , C. Vrahas⁵⁷ , J. Wagner¹⁸ , J. Walsh³³ , E.J. Walton^{1,55} , G. Wan⁶ ,
C. Wang²⁰ , G. Wang⁸ , J. Wang⁶ , J. Wang⁵ , J. Wang⁴ , J. Wang⁷² , M. Wang²⁸ ,
N. W. Wang⁷ , R. Wang⁵³ , X. Wang⁸ , X. Wang⁷⁰ , X. W. Wang⁶⁰ , Y. Wang⁶ ,
Z. Wang¹³ , Z. Wang⁴ , Z. Wang²⁸ , J.A. Ward^{55,1} , M. Waterlaet⁴⁷ , N.K. Watson⁵² ,
D. Websdale⁶⁰ , Y. Wei⁶ , J. Wendel⁷⁹ , B.D.C. Westhenry⁵³ , C. White⁵⁴ ,
M. Whitehead⁵⁸ , E. Whiter⁵² , A.R. Wiederhold⁵⁵ , D. Wiedner¹⁸ , G. Wilkinson⁶² ,
M.K. Wilkinson⁶⁴ , M. Williams⁶³ , M.R.J. Williams⁵⁷ , R. Williams⁵⁴ , Z.
Williams⁵³ , F.F. Wilson⁵⁶ , W. Wislicki⁴⁰ , M. Witek³⁹ , L. Witola²⁰ , C.P. Wong⁶⁶ ,
G. Wormser¹³ , S.A. Wotton⁵⁴ , H. Wu⁶⁷ , J. Wu⁸ , Y. Wu⁶ , Z. Wu⁷ ,
K. Wyllie⁴⁷ , S. Xian⁷⁰ , Z. Xiang⁵ , Y. Xie⁸ , A. Xu³³ , J. Xu⁷ , L. Xu⁴ , L. Xu⁴ ,
M. Xu⁵⁵ , Z. Xu¹¹ , Z. Xu⁷ , Z. Xu⁵ , D. Yang , K. Yang⁶⁰ , S. Yang⁷ ,
X. Yang⁶ , Y. Yang^{27,m} , Z. Yang⁶ , Z. Yang⁶⁵ , V. Yeroshenko¹³ , H. Yeung⁶¹ ,
H. Yin⁸ , C. Y. Yu⁶ , J. Yu⁶⁹ , X. Yuan⁵ , Y. Yuan^{5,7} , E. Zaffaroni⁴⁸ ,
M. Zavertyaev¹⁹ , M. Zdybal³⁹ , F. Zenesini^{23,i} , C. Zeng^{5,7} , M. Zeng⁴ , C. Zhang⁶ ,
D. Zhang⁸ , J. Zhang⁷ , L. Zhang⁴ , S. Zhang⁶⁹ , S. Zhang⁶² , Y. Zhang⁶ , Y. Z.
Zhang⁴ , Y. Zhao²⁰ , A. Zharkova⁴² , A. Zhelezov²⁰ , S. Z. Zheng⁶ , X. Z. Zheng⁴ ,
Y. Zheng⁷ , T. Zhou⁶ , X. Zhou⁸ , Y. Zhou⁷ , V. Zhovkovska⁵⁵ , L. Z. Zhu⁷ ,
X. Zhu⁴ , X. Zhu⁸ , V. Zhukov¹⁶ , J. Zhuo⁴⁶ , Q. Zou^{5,7} , D. Zuliani^{31,p} ,
G. Zunica⁴⁸ .

¹*School of Physics and Astronomy, Monash University, Melbourne, Australia*

²*Centro Brasileiro de Pesquisas Físicas (CBPF), Rio de Janeiro, Brazil*

³*Universidade Federal do Rio de Janeiro (UFRJ), Rio de Janeiro, Brazil*

⁴*Center for High Energy Physics, Tsinghua University, Beijing, China*

⁵*Institute Of High Energy Physics (IHEP), Beijing, China*

⁶*School of Physics State Key Laboratory of Nuclear Physics and Technology, Peking University, Beijing, China*

⁷*University of Chinese Academy of Sciences, Beijing, China*

⁸*Institute of Particle Physics, Central China Normal University, Wuhan, Hubei, China*

⁹*Consejo Nacional de Rectores (CONARE), San Jose, Costa Rica*

¹⁰*Université Savoie Mont Blanc, CNRS, IN2P3-LAPP, Annecy, France*

¹¹*Université Clermont Auvergne, CNRS/IN2P3, LPC, Clermont-Ferrand, France*

¹²*Aix Marseille Univ, CNRS/IN2P3, CPPM, Marseille, France*

¹³*Université Paris-Saclay, CNRS/IN2P3, IJCLab, Orsay, France*

¹⁴*Laboratoire Leprince-Ringuet, CNRS/IN2P3, Ecole Polytechnique, Institut Polytechnique de Paris, Palaiseau, France*

¹⁵*LPNHE, Sorbonne Université, Paris Diderot Sorbonne Paris Cité, CNRS/IN2P3, Paris, France*

¹⁶*I. Physikalisches Institut, RWTH Aachen University, Aachen, Germany*

¹⁷*Universität Bonn - Helmholtz-Institut für Strahlen und Kernphysik, Bonn, Germany*

¹⁸*Fakultät Physik, Technische Universität Dortmund, Dortmund, Germany*

¹⁹*Max-Planck-Institut für Kernphysik (MPIK), Heidelberg, Germany*

²⁰*Physikalisches Institut, Ruprecht-Karls-Universität Heidelberg, Heidelberg, Germany*

²¹*School of Physics, University College Dublin, Dublin, Ireland*

²²*INFN Sezione di Bari, Bari, Italy*

²³*INFN Sezione di Bologna, Bologna, Italy*

²⁴*INFN Sezione di Ferrara, Ferrara, Italy*

²⁵*INFN Sezione di Firenze, Firenze, Italy*

²⁶*INFN Laboratori Nazionali di Frascati, Frascati, Italy*

- ²⁷ INFN Sezione di Genova, Genova, Italy
- ²⁸ INFN Sezione di Milano, Milano, Italy
- ²⁹ INFN Sezione di Milano-Bicocca, Milano, Italy
- ³⁰ INFN Sezione di Cagliari, Monserrato, Italy
- ³¹ INFN Sezione di Padova, Padova, Italy
- ³² INFN Sezione di Perugia, Perugia, Italy
- ³³ INFN Sezione di Pisa, Pisa, Italy
- ³⁴ INFN Sezione di Roma La Sapienza, Roma, Italy
- ³⁵ INFN Sezione di Roma Tor Vergata, Roma, Italy
- ³⁶ Nikhef National Institute for Subatomic Physics, Amsterdam, Netherlands
- ³⁷ Nikhef National Institute for Subatomic Physics and VU University Amsterdam, Amsterdam, Netherlands
- ³⁸ AGH - University of Krakow, Faculty of Physics and Applied Computer Science, Kraków, Poland
- ³⁹ Henryk Niewodniczanski Institute of Nuclear Physics Polish Academy of Sciences, Kraków, Poland
- ⁴⁰ National Center for Nuclear Research (NCBJ), Warsaw, Poland
- ⁴¹ Horia Hulubei National Institute of Physics and Nuclear Engineering, Bucharest-Magurele, Romania
- ⁴² Affiliated with an institute covered by a cooperation agreement with CERN
- ⁴³ DS4DS, La Salle, Universitat Ramon Llull, Barcelona, Spain
- ⁴⁴ ICCUB, Universitat de Barcelona, Barcelona, Spain
- ⁴⁵ Instituto Galego de Física de Altas Enerxías (IGFAE), Universidade de Santiago de Compostela, Santiago de Compostela, Spain
- ⁴⁶ Instituto de Física Corpuscular, Centro Mixto Universidad de Valencia - CSIC, Valencia, Spain
- ⁴⁷ European Organization for Nuclear Research (CERN), Geneva, Switzerland
- ⁴⁸ Institute of Physics, Ecole Polytechnique Fédérale de Lausanne (EPFL), Lausanne, Switzerland
- ⁴⁹ Physik-Institut, Universität Zürich, Zürich, Switzerland
- ⁵⁰ NSC Kharkiv Institute of Physics and Technology (NSC KIPT), Kharkiv, Ukraine
- ⁵¹ Institute for Nuclear Research of the National Academy of Sciences (KINR), Kyiv, Ukraine
- ⁵² School of Physics and Astronomy, University of Birmingham, Birmingham, United Kingdom
- ⁵³ H.H. Wills Physics Laboratory, University of Bristol, Bristol, United Kingdom
- ⁵⁴ Cavendish Laboratory, University of Cambridge, Cambridge, United Kingdom
- ⁵⁵ Department of Physics, University of Warwick, Coventry, United Kingdom
- ⁵⁶ STFC Rutherford Appleton Laboratory, Didcot, United Kingdom
- ⁵⁷ School of Physics and Astronomy, University of Edinburgh, Edinburgh, United Kingdom
- ⁵⁸ School of Physics and Astronomy, University of Glasgow, Glasgow, United Kingdom
- ⁵⁹ Oliver Lodge Laboratory, University of Liverpool, Liverpool, United Kingdom
- ⁶⁰ Imperial College London, London, United Kingdom
- ⁶¹ Department of Physics and Astronomy, University of Manchester, Manchester, United Kingdom
- ⁶² Department of Physics, University of Oxford, Oxford, United Kingdom
- ⁶³ Massachusetts Institute of Technology, Cambridge, MA, United States
- ⁶⁴ University of Cincinnati, Cincinnati, OH, United States
- ⁶⁵ University of Maryland, College Park, MD, United States
- ⁶⁶ Los Alamos National Laboratory (LANL), Los Alamos, NM, United States
- ⁶⁷ Syracuse University, Syracuse, NY, United States
- ⁶⁸ Pontifícia Universidade Católica do Rio de Janeiro (PUC-Rio), Rio de Janeiro, Brazil, associated to ³
- ⁶⁹ School of Physics and Electronics, Hunan University, Changsha City, China, associated to ⁸
- ⁷⁰ Guangdong Provincial Key Laboratory of Nuclear Science, Guangdong-Hong Kong Joint Laboratory of Quantum Matter, Institute of Quantum Matter, South China Normal University, Guangzhou, China, associated to ⁴
- ⁷¹ Lanzhou University, Lanzhou, China, associated to ⁵
- ⁷² School of Physics and Technology, Wuhan University, Wuhan, China, associated to ⁴
- ⁷³ Departamento de Física, Universidad Nacional de Colombia, Bogota, Colombia, associated to ¹⁵
- ⁷⁴ Ruhr Universitaet Bochum, Fakultae f. Physik und Astronomie, Bochum, Germany, associated to ¹⁸
- ⁷⁵ Eotvos Lorand University, Budapest, Hungary, associated to ⁴⁷
- ⁷⁶ Van Swinderen Institute, University of Groningen, Groningen, Netherlands, associated to ³⁶
- ⁷⁷ Universiteit Maastricht, Maastricht, Netherlands, associated to ³⁶
- ⁷⁸ Tadeusz Kosciuszko Cracow University of Technology, Cracow, Poland, associated to ³⁹

- ⁷⁹ *Universidade da Coruña, A Coruna, Spain, associated to* ⁴³
- ⁸⁰ *Department of Physics and Astronomy, Uppsala University, Uppsala, Sweden, associated to* ⁵⁸
- ⁸¹ *University of Michigan, Ann Arbor, MI, United States, associated to* ⁶⁷
- ⁸² *Département de Physique Nucléaire (DPhN), Gif-Sur-Yvette, France*
- ^a *Universidade de Brasília, Brasília, Brazil*
- ^b *Centro Federal de Educação Tecnológica Celso Suckow da Fonseca, Rio De Janeiro, Brazil*
- ^c *Hangzhou Institute for Advanced Study, UCAS, Hangzhou, China*
- ^d *School of Physics and Electronics, Henan University, Kaifeng, China*
- ^e *LIP6, Sorbonne Université, Paris, France*
- ^f *Universidad Nacional Autónoma de Honduras, Tegucigalpa, Honduras*
- ^g *Università di Bari, Bari, Italy*
- ^h *Università di Bergamo, Bergamo, Italy*
- ⁱ *Università di Bologna, Bologna, Italy*
- ^j *Università di Cagliari, Cagliari, Italy*
- ^k *Università di Ferrara, Ferrara, Italy*
- ^l *Università di Firenze, Firenze, Italy*
- ^m *Università di Genova, Genova, Italy*
- ⁿ *Università degli Studi di Milano, Milano, Italy*
- ^o *Università degli Studi di Milano-Bicocca, Milano, Italy*
- ^p *Università di Padova, Padova, Italy*
- ^q *Università di Perugia, Perugia, Italy*
- ^r *Scuola Normale Superiore, Pisa, Italy*
- ^s *Università di Pisa, Pisa, Italy*
- ^t *Università della Basilicata, Potenza, Italy*
- ^u *Università di Roma Tor Vergata, Roma, Italy*
- ^v *Università di Siena, Siena, Italy*
- ^w *Università di Urbino, Urbino, Italy*
- ^x *Universidad de Alcalá, Alcalá de Henares, Spain*
- ^y *Facultad de Ciencias Físicas, Madrid, Spain*
- ^z *Department of Physics/Division of Particle Physics, Lund, Sweden*
- [†] *Deceased*